Improvement in the Functionality & 3D Printability of Pea Protein Gels Prepared by Plasma Activated Microbubble Water

by

Sreelakshmi Chembakasseri Menon

A thesis submitted in partial fulfillment of the requirements for the degree of

Master of Science

in

Food Science and Technology

Department of Agricultural, Food and Nutritional Science
University of Alberta

Abstract

Three-dimensional (3D) food printing is one of the emerging processing technologies that enables the construction of complex food structures and customization. Although various food ingredients have been explored for their 3D printability, pea protein is among the plant proteins that have not been studied extensively on its 3D printability, owing to its native inability to hold shape and structure following extrusion. This study investigated the effect of plasma activated microbubble (PAMB) treatment on the thermal gelation and 3D printability of pea protein isolate (PPI). PAMB treatments with different combinations of discharge gases (80% argon and 20% air, 90% argon and 20% air, 100% argon, and 100% air) were applied to prepare PPI suspensions. These suspensions were then heated at 85°C for 30 and 60 min, followed by immediate cooling to prepare PPI gels. The viscoelastic measurements and mechanical properties of PPI gels indicated that this combined application was suitable for 3D printing, with a notable increase in storage modulus (G'), loss modulus (G'') and compressive strength in PPI-PAMB gels. The 3D printed PPI gels prepared using PAMB treatment exhibited better structure retention, resistance to deformation, and stability during storage. The treatment using PAMB prepared by the combination of argon and air, i.e., 80% argon and 20% air and 90% argon and 10% air, resulted in PPI gels with better rheological properties, mechanical stability and 3D printability. Freeze drying was investigated as a possible post 3D printing processing operation to enhance the shelf life and storage stability of 3D printed PPI gels. The moisture content, water activity and textural properties of the freeze dried 3D printed PPI were investigated. With further studies, freeze dried 3D printed PPI gels can be utilised in protein rich breakfast foods.

Preface

This thesis is an original work done by Sreelakshmi Chembakasseri Menon at the Food Safety and Sustainability Engineering Lab at the University of Alberta under the supervision of Dr. Roopesh Mohandas Syamaladevi.

The thesis consists of five chapters: Chapter 1 provides an introductory overview of the study, including the thesis rationale, hypotheses, and objectives**.** Chapter 2 reviews the scientific literature associated with the studies in Chapters 3 and 4**.** Chapter 3 evaluates the effect of plasma activated microbubble water in improving the functionality and 3D printability of pea protein gels. Chapter 4 describes the application of freeze drying as a post-3D printing process to improve the shelf life of 3D-printed protein gels. Chapter 5 comprises the conclusions of this study and suggestions for future work.

A manuscript based on the study in Chapter 3 "Improvement in the structural properties and 3d printability of pea protein gels prepared by plasma activated microbubble water," has been prepared for submission to an international journal.

Acknowledgment

I want to express my sincere appreciation to Dr. Roopesh Mohandas Syamaladevi for allowing me to join his research laboratory. His unwavering patience, guidance, and motivation helped me successfully navigate my academic and research journey. I sincerely appreciate his dedication and hard work in helping me improve as a student.

I express my profound gratitude to Dr. Lingyun Chen for supporting, guiding, and providing laboratory resources during my research. I sincerely thank Dr. John Wolodko for his contributions as a supervisory committee member, providing me with valuable guidance and feedback. I thank my external examiner, Dr. Feral Temelli, for reviewing my thesis and providing valuable insights that improved my study.

I thank my current and former lab mates for your immense support and help. I want to express my heartfelt appreciation to Harleen Kaur Dhaliwal, who has supported and guided me throughout my academic journey. Her contributions have been precious, and I am grateful for her help. I want to express my deep appreciation to Sitian Zhang and Zhigang Tian for their invaluable assistance in providing me with access to their laboratory resources.

I am immensely grateful to my parents, sister, and all my dear family members who have showered me with their unwavering love, support, and encouragement, owing to which I was able to excel in my academic pursuits. Finally, my heartfelt appreciation goes to my husband, Arun Poduval, who has supported me throughout this long journey. I cannot express enough what his unwavering support has meant to me.

Table of Contents

List of Tables

List of Figures

List of Abbreviations

3D	Three-dimensional
3DFP	Three-dimensional food printing
ACP	Atmospheric cold plasma
DBD	Dielectric barrier
PAMB	Plasma activated microbubble water
PAW	Plasma activated water
PPC	Pea protein concentrate
PPI	Pea protein isolate
RONS	Reactive oxygen-nitrogen species
SEM	Scanning electron microscopy
SPI	Soy protein isolate

Chapter 1 Introduction and objectives

1.1 Introduction

Pea protein has gained significant scientific and commercial attention due to its low cost, high nutritional value, hypoallergenic nature, and availability. Critical functional properties such as solubility, water- and oil-holding capacities, and emulsifying and foaming properties of pea protein have also been deciding factors in its commercial applications (Lam et al., 2018). One of the most relevant food applications of pea protein is for developing meat analogs. Several studies have investigated the production of meat analogs using pea protein and have established it as a promising source of alternate protein (Ferawati et al., 2021; Kaleda et al., 2021). Additionally, studies have revealed that pea protein can be utilized as an adequate ingredient substitute for milk protein (Ben-Harb et al., 2020) and wheat flour (Assad Bustillos et al., 2020). Even though pea protein is widely used as an ingredient in the manufacture of various foods, some specific functionality constraints have limited its utilization in modern food processing technologies (Shanthakumar et al., 2022).

Gelation is one such functional property, that determines the applicability of pea protein in food processing. With a direct relation to the texture of food, the gelation properties of pea protein dictate the feasibility of utilizing pea protein for various processing applications (Lam et al., 2018). Pea protein gelation can be induced by thermal treatment, pH alteration, the addition of salts, and other chemicals (Klost et al., 2020). The inherent properties of native pea protein indicate that it has restricted gelling capabilities, requiring exposure to temperatures exceeding its denaturation temperature of 95°C to form durable gels (Shevkani et al., 2015). However, gelation and structural properties of pea protein have been shown to improve with novel processing technologies. For instance, atmospheric cold plasma treatment can possibly reduce heating temperatures to 80-90°C

for protein gelation, with an improvement in the rheological properties of pea protein gels (Zhang et al., 2021).

Atmospheric Cold Plasma (ACP) is a non-thermal processing technology that is generated by electrical discharge utilizing a variety of input gases and consists of reactive chemical species, such as reactive oxygen and nitrogen species (RONS) (Feizollahi et al., 2020). The existence of these species makes cold plasma useful in various applications such as wastewater treatment, seed germination, food decontamination, inactivation of enzymes, and modification of food properties (Bermudez-Aguirre, 2019). Plasma activated water (PAW) is produced when atmospheric cold plasma interacts with water (Mai-Prochnow et al., 2021). Previous studies showed the utilization of PAW in food processing applications, primarily for disinfection. Bubble-enhanced plasma activation has been developed to improve the efficiency of plasma activation in water, utilizing tiny bubbles to entrap and release plasma reactive species into the water (Gao et al., 2022a).

Three-dimensional (3D) food printing is an applied version of additive manufacturing technology that converts a computer-generated 3D model into an edible object, utilizing food materials as printing inks (Yu et al., 2022). Advantages of 3D food printing include food personalization, customization, and precise nutrition control (Lipton, 2017). Even though there are several techniques in 3D food printing, extrusion printing, which works on the principle of extruding the food material through a fine nozzle to form a layer-by-layer structure is the most commonly researched method (Zhang et al., 2022). Various printable and traditionally non-printable materials have been studied for 3D food printing. While natively printable materials undergo 3D food printing with minimal preprocessing and pre-treatment, traditionally non-printable materials undergo several pre-processing, with or without additives, before 3D printing (Dankar et al., 2018). Although pea protein has nutritional value, functional properties, and low allergenicity, it has

limited application in 3D food printing despite being a highly researched alternative protein. It is rarely used as a major ingredient in 3D food printing studies, with most focusing on its role as an additive to improve printability. No studies have explored its potential as a primary ingredient in 3D food printing or any post-3D printing processing to improve its shelf-life stability. With the use of novel pre-treatments, i.e., by using ACP or PAW, gelation properties and printability of pea protein can be possibly improved, though studies focusing on the application of these technologies are limited or not available.

1.2 Hypothesis

The overall hypothesis of this research was that cold plasma technology can significantly enhance the gelation properties of pea protein isolates, which would ultimately lead to improved utilization in novel processing methods such as 3D food printing.

Introducing microbubbles in plasma activated water can enhance the efficacy of cold plasma. The effectiveness of plasma activated microbubble water will depend on the plasma treatment time and the feed gas utilized for plasma generation. The plasma reactive species in plasma activated microbubble water can interact with plant proteins to improve their gelation properties. The resultant pea protein gels with superior gelation and viscoelastic properties can be utilized in 3D food printing, leading to substantial improvements in the quality of 3D-printed pea protein. With the utilization of plasma activated microbubble water, 3D-printed pea protein gels will demonstrate improved deformation resistance and storage stability for 3D printing.

1.3 Objectives

The overall objective of this research was to evaluate the applicability of plasma activated water microbubble technology on thermal gelation, rheological behavior, mechanical properties, and 3D printability of pea protein gels. The specific objectives were to:

i. Design a set of pre-treatment protocols to utilize pea protein isolate as a food ink for 3D printing (Chapter 3).
ii. Standardise a time-temperature combination for heat gelation of pea protein suspension made from plasma activated microbubble water (Chapter 3).
iii. Evaluate the effect of feed gas compositions of argon and air in the characterization of reactive species, gelation, and 3D printability of pea protein (Chapter 3).
iv. Evaluate the rheological properties and 3D printability of pea protein as a sole ingredient in food ink (Chapter 3).
v. Assess the storage stability and deformation stability of 3D-printed pea protein isolates (Chapter 3).
vi. Evaluate the structure and textural properties of freeze dried 3D-printed pea protein gels (Chapter 4).

This research focused on applying plasma activated water to improve the functionality of pea protein to be utilized in novel food processing technologies. Pea protein was selected for this research due to its emerging importance as an alternative protein. Pea protein isolate, a highly purified version of pea protein, was selected to assess the effect of plasma activated water. This research used a bubble spark discharge cold plasma generation system to produce plasma activated microbubble water. An extrusion 3D printer was utilized in this research to print a 3D printed structure.

Chapter 2 Literature review

2.1 Plant Proteins and its gaining popularity

Plant proteins are complex structures, comprising sequences of numerous amino acids, which contribute to the growth and development of plants. The unique combination of amino acids in each plant protein determines its specific function and nutritional value. Crops such as cereals, legumes, and pulses are the chief source of plant proteins, with each source of protein exhibiting a wide variety of structures and functionalities (Arif and Pauls, 2018). Plant proteins have been utilised in major applications such as food processing, agriculture, biofuels, bioproducts, and biopharmaceuticals (Wadhave et al., 2014)

Plant protein applications in the food industry have increased over the past decade, with growing demand for sustainable meat alternatives. The global trend towards clean-label products and better considerations on animal welfare have shown a shift towards a plant-based diet (Munialo, 2023). Secondly, peak interest in high-protein foods, particularly those with specific functional properties has led to incorporating plant proteins as a primary ingredient in various food products (Małecki et al., 2021). Additionally, with more consumers choosing to adopt healthier dietary habits, it is essential to alter their food preferences, by incorporating plant-based protein (Detzel et al., 2022).

Numerous plant protein sources such as peanuts, soybeans, kidney beans, rice, quinoa, sunflowers, cottonseed, camelina, maize, fava bean, oat, and peas have been researched for their possible food processing applications (Kumar et al., 2022; Małecki et al., 2021; Munialo, 2023; Xiao et al., 2023). However, out of all the plant proteins, considerable research interests are concentrated in legume protein. The application of legume proteins such as soy protein isolate (SPI) and pea

protein isolate (PPI) has been studied widely for possible techno-functional property improvement in food products (Omura et al., 2021).

Legume proteins have challenges in food processing due to poor solubility, limited functionality, and anti-nutritional factors that affect digestibility. Most legume proteins, in their native form, exhibit numerous challenges in food product development. Reduced solubility and dispersibility, presence of anti-nutritional factors, and limited functionalities are some of the few challenges, that inhibit the full-scale application of these proteins in food processing despite having numerous commercial and therapeutic benefits (Sim et al., 2021). Hence, most present-day scientific research in this field focuses on possible modification and alteration of legume proteins to bring out improved physicochemical properties and structural properties, with a reduction of anti-nutritional factors. Several processing techniques such as cooking, autoclaving, germination, microwave processing, irradiation, fermentation, and extrusion have been investigated to improve plant protein quality and functionality (Kumar et al., 2022; Park et al., 2010; Sá et al., 2019).

2.1.1 Pea protein - Overview

Pea protein, derived from yellow field pea (*Pisum sativum*), is an emerging legume protein, which can be a potential alternative to animal protein owing to its nutritional value, functional properties, and low allergenicity (Owusu-Ansah and Mc curdy, 1991). As of 2021, Canada has a production of 2.25 million tons of dry peas (FAOSTAT, 2023). According to Statistics Canada, this has further increased to 3.24 million tons in 2022, thereby making Canada as the world's largest producer of field peas, followed by Russia and China. Canada is also leading the dry pea market with an expected export of 2.65 million tons in 2023, indicating that around 80% of dry peas produced in Canada is exported. The domestic consumption of dry pea inside Canada is seen increasing from

580 thousand tons (2021-2022) to 697 thousand tons (2022-2023), indicating an increased demand in pea protein inside Canada(Statistics Canada, 2023)

The peas contain two main protein fractions, namely, albumins and globulins. Albumins account for 10-20% of the total protein, while globulins for 70-80%. Prolamines and Glutelins are also present in pea protein in minor amounts. Globular proteins account for major storage proteins in pea, such as legumin (11S), vicilin (7S) and convicilin (Rubio et al., 2013). The globulin fraction of pea protein is high in specific amino acids such as arginine, phenylalanine, leucine, and isoleucine, while the albumin fraction contains higher quantities of tryptophan, lysine, and threonine. As is the case with most legumes, pea protein lacks the essential amino acid methionine and non-essential amino acid, cysteine (Owusu-Ansah and Mc curdy, 1991)

Pea proteins are majorly utilized as a techno-functional ingredient aimed to enhance the characteristics of final food products, it has excellent properties such as solubility, water- and oil-holding capacities, emulsifying, foaming, and gelling properties. Physical, chemical, and enzymatic treatments can further improve these functional properties to expand food applications of pea proteins (Lam et al., 2018).

2.1.2 Food applications of pea proteins

Pea proteins have recently emerged as a potential protein, which can be utilized in the development of meat analogs. Several studies have investigated the production of meat analogs using pea protein.

Xia et al. (2022) reported that adding *Haematococcus pluvialis* residue and pea protein improves texture and appearance in meat analogs. Another study investigated the feasibility of oat and pea protein blends for preparing meat analogs and established that these blends can be utilized as

alternatives to gluten and soy proteins (Kaleda et al., 2021). Similarly, the functionality of yellow bean and faba bean protein isolates was evaluated for possibilities to develop meat alternatives (Ferawati et al., 2021). The water-holding capacity and protein content affect meat analog's texture properties. Also, protein isolation techniques can influence the texture of the final product. For instance, dry separation of pea proteins, which includes a combination of ultrafine milling, air-classification, and electromagnetic separation results in a porous and soft meat analog. In contrast, wet separation using isoelectric point precipitation produces a solid-like texture due to enhanced foaming and emulsification properties (Zhu et al., 2021).

Studies have also shown that pea protein can be utilized as an effective substitute in various food products. For example, milk gels produced with the partial substitution of milk protein with pea protein (50%) were perceived as a dairy product with a distinct cheesy aroma (Ben-Harb et al., 2020). Pea protein isolate (PPI) has also been utilized to improve the stability of cake batter, with a partial substitute of wheat flour in the batter (Assad Bustillos et al., 2020). Other food applications of pea protein include utilization for encapsulation of various bioactive ingredients, such as vitamin D, vitamin C, curcumin, flaxseed oil, lycopene, and probiotic bacteria, in modified PPI complexes. Studies have shown that PPI helps in encapsulation stability and improves bioavailability of the encapsulated material (Ge et al., 2020).

2.1.3 Functionality improvement in pea protein

Numerous research studies focused on the functionality improvement of pea protein by applying novel technologies. Fundamental functional properties of pea protein, such as foaming capacity, emulsification, water-holding capacity, and gelation have been investigated for their possible enhancement. It was found that freezing and freeze-thaw cycling treatments have enhanced pea protein properties such as fat absorption capacity, water holding capacity, foam stability index, and

emulsion stability index (Kumar et al., 2022). Co-spray drying is another emerging technology employed to induce conformational changes and modify surface charge in pea protein isolates. Co-spray drying of pea protein with trehalose, sucrose, and sodium hexametaphosphate resulted in improved solubility, thermal properties, emulsification, and foaming capacity as well as stability (Cui et al., 2021), while pea protein co-spray drying with cyclodextrins reduced its beany flavor (Cui et al., 2020). A modification in the secondary and tertiary structure of pea protein fraction using high-intensity ultrasound treatment has led to improved solubility and foaming stability (Gao et al., 2022).

The application of novel technologies such as ohmic heating, high-pressure processing, shear cell technology, ultrasound, pulsed electric fields, irradiation, filtration, supercritical carbon dioxide, and cold plasma technology is presently being investigated for possible functionality improvement of plant proteins. Ohmic heating, cold plasma, ultrasound and pulsed electric field treatments induce protein denaturation and modification, potentially improving protein functionality and solubility. High pressure processing, irradiation and filtration can enhance the texture and shelf life of plant proteins, while retaining their nutritional value. (Avelar et al., 2021; Lam et al., 2018; Mirmoghtadaie et al., 2016; Omura et al., 2021). While some these technologies alter protein structure and properties, these technologies would also impact gelation, solubility, stability, crosslinking density, water-holding capacity, hydrophobicity, strength, and viscoelasticity.

2.1.4 Gelation properties of pea protein

Globulins, a significant class of plant proteins found in legumes like soy and peas can form gels when heated. This process, termed gelation can vary depending on specific protein sources and extraction methods. Gelation in plant proteins is characterized by an increase in storage modulus

(G') over loss modulus (G”) and is an essential functional property (Nicolai and Chassenieux, 2019).

Gelation of pea protein can be initiated through various methods such as thermal treatment, alteration of pH, addition of salts, and other materials, such as transglutaminase, hydrocolloids like guar gum or xanthan gum (Klost et al., 2020). Thermal gelation is the most widely used gelation technique in protein. When pea protein is heated to higher temperatures, the proteins denature and then bonds upon cooling, resulting in gel formation. For thermal gelation, pea protein can only create strong gels when exposed to temperatures higher than its denaturation temperature of 95°C, exhibiting gels with good mechanical strength and viscoelasticity (Zhang et al., 2021a). A key disadvantage with thermal gelation is the potential loss of nutritional value due to the application of high temperatures.

Alteration of pH of protein solution can influence its gelation behavior (Zhu et al., 2021). Pea proteins have different isoelectric points and gelation can be promoted by adjusting the pH to be either above or below this point. Addition of salts, such as calcium chloride or sodium chloride, can also induce gelation in pea protein solutions, leading to the formation of a protein network (Tanger et al., 2022). Enzymes like transglutaminase can be used to crosslink pea proteins, enhancing their gelation properties through covalent bonds between protein molecules (Wang et al., 2022). Even though these techniques have been utilised for gelation of pea proteins, potential changes in sensory attributes of proteins limits its applicability..

Gelation properties of pea protein can also be improved with the application of processing technologies such as ultrafiltration, salt extraction, micellar precipitation, atmospheric cold plasma, and high-intensity ultrasound treatment (Klost et al., 2020).

2.2 Cold plasma technology

Plasma is the fourth state of matter, which consists of highly electrically conductive, partially ionized substances. Cold plasma is the energized state of a gas at ambient temperature and atmospheric pressure, and it has various applications in food production and processing. An electrical discharge generates cold plasma by utilizing a variety of input gases, such as air, helium, nitrogen, and argon (Gao et al., 2022a). The generated plasma predominantly consists of reactive chemical species, such as reactive oxygen and nitrogen species (RONS) (Feizollahi et al., 2020). Owing to the presence of these reactive species, plasma technology has numerous applications in the food industry, including wastewater treatment, seed germination, food decontamination, inactivation of enzymes, and modification of key functional properties of food and packaging properties and protein functionality improvement (Bermudez-Aguirre, 2019a; Rao et al., 2023). Cold plasma treatment was able to improve the gelation properties of PPI, with a potential of protein gelation at 80-90°C temperature range (Zhang et al., 2021) as well as emulsification and other functional properties of pea protein (Bu et al., 2023)

Standard methods of cold plasma generation include corona discharge (jet discharge), dielectric barrier discharge, and microwave-induced discharge. The occurrence of corona discharge is typically limited to an electrical field that is not uniform, which is created by administering a high voltage of approximately 10-20 kV. In contrast, in dielectric barrier discharge, dielectric materials such as quartz, glass, silicon rubber, or plastics are placed between two electrodes, within which plasma is generated when a high voltage is applied. Microwave plasma is induced by the pulsed microwave, which is then injected into the sample to be treated (Gao et al., 2022a).

2.2.1 Plasma activated water (PAW)

Cold plasma technology is versatile and can be customized based on specific needs using feed gas and plasma source design. When interacting with liquids, atmospheric plasma creates plasma activated liquids. Plasma activated water (PAW) is the most studied plasma activated liquid (Mai-Prochnow et al., 2021). Typically, PAW generated from atmospheric cold plasma contains high levels of RONS, such as hydroxyl radicals, hydrogen peroxide, ozone, superoxide, nitric oxide, and peroxynitrite. The presence of RONS can significantly alter the physiochemical properties of PAW, leading to an increase in conductivity, redox potential, and acidity with a decrease in pH (Gao et al., 2022a).

The PAW generation has numerous applications in the food industry. For instance, PAW was utilized for sanitation and disinfection (Gao et al., 2022a), biofilm removal (Mai-Prochnow et al., 2021), wastewater treatment, bacterial inactivation of fruits and vegetables (Soni et al., 2021), accelerated seed germination (Feizollahi et al., 2023), plant disease control (Guo et al., 2021), improvement in the shelf life of foods (Misra et al., 2019) and reduction in pesticide residue in fresh produce. (Gao et al., 2022a).

2.2.2 Microbubbles in PAW and applications

Even though cold plasma and plasma activated water have been proven to be effective non-thermal techniques for a variety of applications, it is generally regarded that the efficiency of plasma activation in water can be low, as the gas-liquid interface only allows a limited number of reactive species to penetrate and interact with the intended molecules (Gao et al., 2022b). Bubble-enhanced plasma activation has been developed to combat this challenge. This method utilizes microbubbles, with diameters between 1 and 100 micrometers, characterized by high mass transfer efficiency and

dissolution rate, a high surface-to-volume ratio, and extended residence time in liquid to combine with plasma during generation. This ensures that the generated gaseous plasma is contained within the bubbles and is effectively transferred to water through these bubbles. This confinement of gaseous plasma species inside the bubbles, followed by the introduction of these bubbles into the water results in better agitation and mixing of plasma reactive species with water and their improved interactions with the target molecules (Gao et al., 2022b).

Although this is a recent technological advancement, it has been demonstrated that plasma activated microbubbles have effective antimicrobial activity on *Klebsiella michiganensis* present on the inner surfaces of PVC pipes, with a reduction of 3.1 log CFU/cm^2(Xu and Tan, 2023). Another study utilized plasma activated microbubble water on *Enterococcus faecalis* biofilm and demonstrated that with a combination of ultrafiltration treatment, the microbubbles display significant disinfection and biofilm removal effects (Zhu et al., 2023). However, no previous studies reported the utilization of plasma activated microbubble (PAMB) water with different feed gases to improve the functionality of plant proteins.

2.3 Three-dimensional food printing (3DFP)

3D printing is an additive manufacturing technology that utilises digital models built through computer-aided design software to construct 3D objects using a 3D printer. Printing is executed by stacking materials layer-over-layer in a three-dimensional space. In other words, 3D printing creates 3D objects by layering materials based on a digital model. This novel technology has evolved to be vitally crucial across multiple spheres of life, with widespread applications in various industries, such as construction, manufacturing, healthcare, and education (Jiang et al., 2022; Li et al., 2021; Yu et al., 2022).

3D food printing is an applied version of additive manufacturing technology that converts a 3D computer model into an edible object using food materials as inks. Creating a 3D printed food initiates with developing a three-dimensional model using computer aided design software. The output of this software, a model file (.stl format), is subsequently transferred into another software (slicing software), which generates a G-code. This G-code is then introduced to a 3D food printer to print the desired shape (Mantihal et al., 2020). The possibilities of personalization, customization, and construction of complex shapes with 3DFP are deciding factors leading to the increased popularity of this technology (Lipton, 2017). With the added advantages of precise nutrition control and the possibility of reducing food wastage using food by-products, the scientific world is keenly interested in this technology (Kim et al., 2018).

2.3.1 3D food printing methods

The printability and construction of food shapes in 3D food printing depends on several factors, such as printing method, type of printer, properties of food inks, and application of post-processing methods. Different 3D food printing methods have been developed, including extrusion printing, selective laser printing, and binder jetting (Mantihal et al., 2020).

The process of binder jetting entails the controlled binding of a powdered substance with a liquid binder, along with the application of successive layers of powder to produce a 3D object. Software and an infrared laser are used in laser sintering. The laser is directed onto a scanner, which reflects the beam onto the printer bed where the powdered material is located. This process results in a precise and solid structure formed through sintering (Godoi et al., 2018). The most commonly used technique for 3D food printing is extrusion printing. It operates by pushing food material (also known as food inks) through a thin nozzle to create a layer-by-layer design on the printing bed (Zhang et al., 2022).

While applying the extrusion method to 3D printing, the food materials must be of a semi-solid or viscous nature. This ensures easy extrusion through the nozzles of the 3D printer syringe. In order to obtain a perfect 3D extruded food product, the material properties, including thermal properties, rheology, and mechanical properties of food inks need to be identified before utilizing them for 3D food printing (Mantihal et al., 2020).

2.3.2 Food materials used in 3D printing

Dankar et al. (2018) broadly classified food materials utilized in 3D extrusion printing into printable materials, non-printable traditional food materials, and alternate ingredients. Printable food inks can be easily extruded through a printer nozzle without any pre-processing or treatment to aid extrusion. Foods such as chocolate, hummus, and dairy pastes are some of the printable food inks that have been demonstrated to form stable 3D-printed shapes (Le Tohic et al., 2018; Liu et al., 2018, 2019; Mantihal et al., 2019; Severini et al., 2016).

Most foods fall in the second category of non-printable traditional food materials. These food materials cannot be extruded through a printer nozzle in their native form; therefore, they require additional processing steps, additives, or other minor ingredients to convert these into printable inks. Owing to this, many scientific studies are evaluating the possibilities of converting natively non-extrudable foods and other novel food ingredients into stable 3D-printed structures (Voon et al., 2019). Alternative ingredients are those food products that are not conventionally utilized for consumption. These include byproducts of food processing, residues from agricultural processes, and nutritionally rich ingredients, which have a cultural stigma associated with them, such as insect protein (Dankar et al., 2018).

Table 2.1 lists major food inks utilized in 3D food printing in the past few years. Even with vast scientific studies on possible food inks for 3D food printing, many food products with fundamental functional and nutritional properties have not been explored for possible pretreatment or modification to fit into 3D food printing.

Table 2.1 List of major food products/ingredients utilized in 3D printing and corresponding minor ingredients and additives.

Major ingredients	Minor ingredients and additives	Reference
Chocolate	Cranberry powder and methylcellulose	Hao et al. (2019)
Chocolate	Magnesium stearate	Mantihal et al. (2019)
Baking dough	None	Yang et al. (2018)
Baking dough	*Lactobacillus plantarum* and Calcium caseinate	Zhang et al. (2018)
Baking dough	Pea protein isolate	Hussain et al. (2021)
Milk protein concentrate	Whey protein concentrate	Liu et al. (2018)
Instant milk powders	None	Lille et al. (2018)
Processed cheese	None	Le Tohic et al. (2018)
Mashed potato	Potato starch and trehalose	Liu et al. (2018)

Vegetable powders (broccoli, carrot, spinach)	Hydrocolloids - hydroxypropyl methylcellulose, locust bean gum, Xanthan gum, and Guar gum	Kim et al. (2018)
Banana paste	Pea protein isolate	Kim et al. (2021)
Beetroot	Pumpkin powder soy protein isolate	Phuhongsung et al. (2020)
Potato starch	Pea protein, butter	Chuanxing et al. (2018)
Maize starch	None	Lille et al. (2018)
Cellulose nano fiber	Maize starch, Instant milk powder	Lille et al. (2018)
Protein and fibre rich foods (rye bran, oat protein concentrate, faba bean protein concentrate)	None	Lille et al. (2018)
Wheat based gels – flour, starch, meal	None	Zheng et al. (2021)
Soy protein isolate	Sodium alginate and gelatin;	Chen et al. (2019)
Texturized soy protein	hydrocolloids- Xanthan gum/ konjac gum/ sodium alginate/ guar gum/ sodium carboxymethyl cellulose/ hydroxyethyl cellulose	Chen et al. (2021)

2.3.3 Application of pea protein in 3D food printing

Despite being a highly researched alternative protein with abundant nutritional value, functional properties, and low allergenicity, pea protein application in 3D food printing is observed to be very limited. Most 3D food printing studies involving pea protein reported its usage as a minor ingredient (1%-20%). Table 2.2 lists the studies on 3D printing of pea proteins. It can be observed that much focus is concentrated on studying the role of pea protein in improving the printability

of other foods, with no studies focusing on pea protein as a significant ingredient for possible 3D printing. This area requires a lot more research as 3D printing of pea proteins has a lot of scope in food applications. There is a possibility of custom designing, with specific nutrients and novel structures using pea proteins. Moreover, novel techniques such as encapsulation can also be utilized, along with 3D printing.

Table 2.2 Current application of pea protein in 3D food printing

Applications	Key points	Reference
Maillard reaction product of xylose–pea protein enzymatic hydrolysate (xMPR)	Potato starch + 1% Pea Protein+ diluted xMPR was gelatinized and 3D printed.	Zhou et al. (2020)
Different blend ratios of alginate and pea protein solutions	The alginate-pea protein solution (80:20) displayed optimum printability and was used for	Oyinloye and Yoon (2021)

	additive-layer manufacturing simulation to investigate the optimum printing conditions.	
Jammed oil-in-water emulsion with pea protein particles	pH-adjusted pea protein particles incorporated into the jammed emulsion exhibit elastoplastic rheology, creating an edible 3D printable material.	Sridharan et al. (2021)
Porcine plasma protein and pea protein concentrate blended dough with glycerol.	Determination of the rheological properties required for 3D printing protein-based dough. Biopolymer/ Glycerol ratio for printability- 45%. Biopolymer composition (PPP 90%, PPC 10%).	Álvarez-Castillo et al. (2021)
Edible pickering emulsions stabilized by pea protein isolate-high methoxyl pectin-epigallocatechin gallate (PPI-HMP-EGCG) complexes.	Pickering emulsions stabilized by the PPI-HMP-EGCG complex and cinnamaldehyde were successfully 3D printed.	Feng et al. (2022)

2.4 Freeze drying of foods

Freeze drying is a popular method of preserving food that eliminates moisture from frozen foods by exposing them to low temperature and pressure conditions. The process involves freezing and placing the food in a vacuum, where the ice crystals are converted to water vapor through sublimation (Nowak and Jakubczyk, 2020). Foods retain texture, flavor, and nutritional value after freeze drying while extending their shelf life. Preserving delicate foods like fruits and vegetables

is best achieved through freeze drying. This method eliminates the harm caused by heat-based treatments such as canning or dehydration (Majumdar, 2007). Studies on freeze drying of fruits such as oranges (Silva-Espinoza et al., 2020), blueberries (Munzenmayer et al., 2020), blackberries (Franceschinis et al., 2014), guava, papaya (Hawlader et al., 2006), and strawberries (Meda and Ratti, 2005) as well as vegetables such as carrot (Regier et al., 2005), pumpkin, (Ciurzyńska et al., 2014; Guiné and Barroca, 2012) peppers (Guiné and Barroca, 2012) and asparagus (Nindo et al., 2003) have been reported in the last decades.

Proteins such as soy protein isolate/κ-carrageenan hydrogels (Yang et al., 2022), whey protein hydrogels (Manzocco et al., 2021), chickpea protein isolates (Kaur and Singh, 2007) and quince seed gum (Ahmadzadeh-Hashemi et al., 2023) have been studied for freeze drying. Similarly, Pea protein isolates have also been investigated for freeze and spray drying on the interface and foam stabilizing properties (Yang et al., 2022).

2.4.1 Freeze drying of 3D-printed foods

Some foods like chocolate can be considered ready to consume post-printing. Many 3D-printed foods may need further steps to ensure safety for consumption (Dankar et al., 2018). Baking, boiling, or frying are some of the traditional food processing techniques, that can be utilized as a post-printing technique. However, most of these techniques essentially result in various altered textural properties and physical alterations. Even though an alteration in textural properties might be considered agreeable in some instances, there are times when it is not agreeable with the final desired product quality. Moreover, traditional cooking can also lead to chemical changes such as protein denaturation, water loss, evaporation, and changes in color, volume, and nutritional value (Sun et al., 2018).

It has been demonstrated that freeze drying is less intensive than oven-drying or spray-drying, even though it may cause specific changes in texture and mechanical properties (Bhatta et al., 2020). This significant observation has led to the application of freeze drying to non-traditional food sources in the last few years. A comparison study was made between oven and freeze drying, two post-3D printing techniques to determine their efficacy in preserving shape stability and texture (Dankar et al., 2018). This study found that freeze drying was better at maintaining the 3D-printed structure than oven-drying. With an increased hardness and dry matter content, freeze dried food had a solid structure, unlike its oven-dried counterpart (Dankar et al., 2018).

Another study involving the drying of 3D printed pumpkin snacks found that freeze drying had a significant impact on the crispness of the snack (Chen et al., 2022). Another study, which involved encapsulation of probiotics using a combination of 3D printing and freeze drying, noted that the 3D printed products transformed a semi-solid to a solid-like state after freeze drying, as confirmed by increased hardness and decreased water activity, demonstrating a potential to produce shelf-stable supplement food (Kuo et al., 2022)

2.5 Summary

The literature review has revealed that a limited number of studies have evaluated the application of pea protein isolate as a potential primary ingredient for 3D food printing. It can be assumed that these lacunae may be attributed to the inherent functional properties of the pea protein that do not support 3D food printing. These research lacunae are addressed in Chapter 3 of this thesis, where plasma activated microbubbles have been utilized to improve gelation and 3D printability of pea protein. Chapter 4 of this thesis further extends the studies on 3D printed pea protein isolates, studying the scope of freeze drying as a potential post-processing technology for adequate storage, shelf stability, and nutrition preservation of 3D printed pea protein gels.

Chapter 3 Improvement in the structural properties and 3D printability of pea protein gels prepared by plasma activated microbubble water

3.1 Introduction

Pea protein is a plant protein that has gained a lot of scientific and commercial interest owing to its high nutritional value, low cost, availability, and hypoallergenic nature. Salt-soluble globulin proteins comprise the major portion of pea proteins, followed by water-soluble albumin proteins (Lam et al., 2018). Pea proteins have been used to produce foods such as bread, cereals, extruded snacks, non-dairy beverages, and meat analogs (Lam et al., 2018; Sim et al., 2021; Xiao et al., 2023). However, the challenges associated with the functionality improvement of pea proteins have limited the use of pea protein as a primary food ingredient in modern food processing technologies (Shanthakumar et al., 2022). Gelation is one such functional property that determines the applicability of pea protein in food processing, owing to its effect on food texture (Lam et al., 2018). Pea protein gelation can be induced by thermal treatment, pH alteration, the addition of salts, and other chemicals (Klost et al., 2020). Strong gels can only be formed by native pea protein at temperatures exceeding its denaturation temperature of 95°C despite having gelling properties (Shevkani et al., 2015). Improving the functional properties of plant proteins through thermal gelation, chemical cross-linking, or a combination of both are some of the most widely researched methods in these natively non-extrudable food products (Pérez et al., 2019).

Non-thermal (cold) plasma is an emerging technology that is generated by an electrical discharge by utilizing a variety of input gases. This potentially cost-effective, sustainable, and chemical-free technology is currently under research for various applications in the food industry (Bermudez-Aguirre, 2019a). For instance, cold plasma technology has been widely studied for its applications in wastewater treatment, seed germination, microbial inactivation, and protein functionality improvement (Rao et al., 2023). Plasma produces reactive oxygen species (ROS) and reactive

nitrogen species (RNS) (Feizollahi et al., 2020). Cold plasma treatments have been shown to improve protein gelation. Treatments using atmospheric pressure plasma jet, dielectric barrier discharge, and nanosecond pulsed discharge have resulted in enhanced gelation properties of pea protein (Bu et al., 2023). By direct atmospheric cold plasma treatment of pea protein isolate, the heating temperature for pea protein gelation was brought down to 70-80°C (Zhang et al., 2021). A similar reduction in heating temperature for protein gelation can also be obtained with indirect plasma treatment using plasma activated water bubbles. Plasma generation and activation in underwater bubbles is a recent development in plasma application. Confinement of gaseous plasma inside the bubbles, followed by the introduction of these bubbles into the water, results in better agitation and mixing of plasma reactive species with water and their improved interactions with the target molecules (Gao et al., 2022).

Three-dimensional (3D) printing, also known as additive manufacturing technology, is a construction method that relies on digital models that are built through computer-aided design software to produce 3D objects using a 3D printer by stacking materials layer-over-layer in a three-dimensional space (Yu et al.,2022; Li et al.,2021; Jiang et al.,2022). The possibilities of personalization, customization, and construction of complex shapes have led to an increase in scientific interest in 3D food printing. The advantages of precise nutrition control and reduction of food wastage further increased the popularity of this technology (Lipton, 2017; Kim et al., 2017). The most common technology used for 3D printed foods is extrusion printing, which works on the principle of extruding the “food inks” through a fine nozzle to form a layer-by-layer structure on the printing bed (Zhang et al., 2022). A variety of food materials such as mashed potato (Chuanxing et al., 2018), vegetable powder (Kim et al., 2018), fruit pastes (Kim et al., 2021), fiber-enriched foods such as starch and cellulose nanofiber, protein-enriched foods such as oat protein and faba

bean protein (Lille et al., 2018), and soy protein (Yu et al., 2022) have been evaluated for their suitability for 3D food printing. Chocolate, dairy, and dough are some of the natively extrudable food inks that have been demonstrated to form stable 3D printed shapes (Liu et al., 2018; Mantihal et al., 2019; Severini et al., 2016; Le Tohic et al., 2018; Liu et al., 2019). Pea protein gels can be possibly used for 3D food printing applications, including the preparation of plant-based meat or cheese analogs, encapsulation, and delivery of bioactive and nutritional compounds. However, as a natively non-extrudable food material, pea proteins have not been utilized as a major component in 3D printing.

Scientific and commercial interests are driving the research on evaluating the possibilities of converting natively non-extrudable foods and other novel food ingredients into stable 3D printed structures (Voon et al., 2019). A limited number of studies are available in the literature on the application of plasma activation for improving the functional properties of plant proteins (Bu et al., 2023). Even though the gelation of pea proteins has been widely researched (Klost et al., 2020), there is no previous research that has investigated the effect of plasma activated bubbles in the improvement of gelation properties, such as reduction in heating temperature or increase in viscoelastic properties of gels. While there are certain studies on 3D food printing that utilizes pea protein as a functional additive for improving the printability of potato starch and banana (Chuanxing et al., 2018; Kim et al., 2021), there is no previous research, that studied the feasibility of applying pea protein as a major component in 3D food printing.

It was hypothesized that the 3D printability of pea proteins could be improved with a combined application of cold plasma and thermal gelation. This research aimed to investigate the applicability of plasma activated water microbubble technology on thermal gelation, rheological behavior, mechanical properties, and 3D printability of pea protein gels. The outcomes of this

research will help to understand the potential applicability of pea protein as a food ink for 3D food printing.

3.2 Materials and methods

3.2.1 Raw material

Pea protein isolate was purchased from a local store (Bulk Barn, Edmonton), and proximate analysis was conducted to determine the chemical composition. The protein content was analyzed with LICO, and the ash content was analyzed using oven drying. The protein content of the sample was determined at 83.0 ± 0.15 %, with a moisture content of 6.6 ± 0.09 %, ash content of 7.0 ± 0.13 %, and carbohydrate content of 6.7 ± 0.19 %, and no traces of crude fat.

3.2.2 Plasma activated microbubble water preparation

Plasma activated microbubbles (PAMB) in water were produced using a bubble spark discharge reactor. The reactor (Fig 1A) consisted of a stainless-steel rod of 5 mm diameter, which served as the high-voltage electrode and was encased into a quartz tube (15 mm inner diameter). The quartz tube had ten holes, each having a diameter of 500 μm, that were uniformly distributed around the base, to allow gas to flow through the tube and produce microbubbles and diffuse into distilled water. A distance of 10 mm was maintained between the high-voltage electrode and the holes of the quartz tube. Another stainless steel rod with a 5 mm diameter was used as a ground electrode. Both the quartz tube encasing the high voltage electrode and the ground electrode were submerged into the glass beaker containing distilled water in such a manner that they touched the bottom of the beaker. The high voltage was supplied to the electrode through a transformer and plasma generator (Leap100, PlasmaLeap Technologies, Sydney, Australia), capable of discharging power of 0–400 W at an AC frequency of 50 Hz–3000 Hz. The gas flow into the reactor was controlled by a mass controller (MC-Series, Alicat Scientific, Tucson, AZ, USA) and was fixed at 1 SLPM

(Standard Litre Per Minute). The reactor was operated at fixed parameters in all experiments (resonance frequency – 60 kHz; discharge frequency – 1000 Hz; duty cycle – 66 µsec; input voltage – 150 V).

The PAMB water was prepared by treating 100 ml distilled water continuously for 30 min in a 250 ml beaker at room temperature (20°C-23°C) using the bubble spark discharge reactor, with different combinations of air and argon as feed gases.

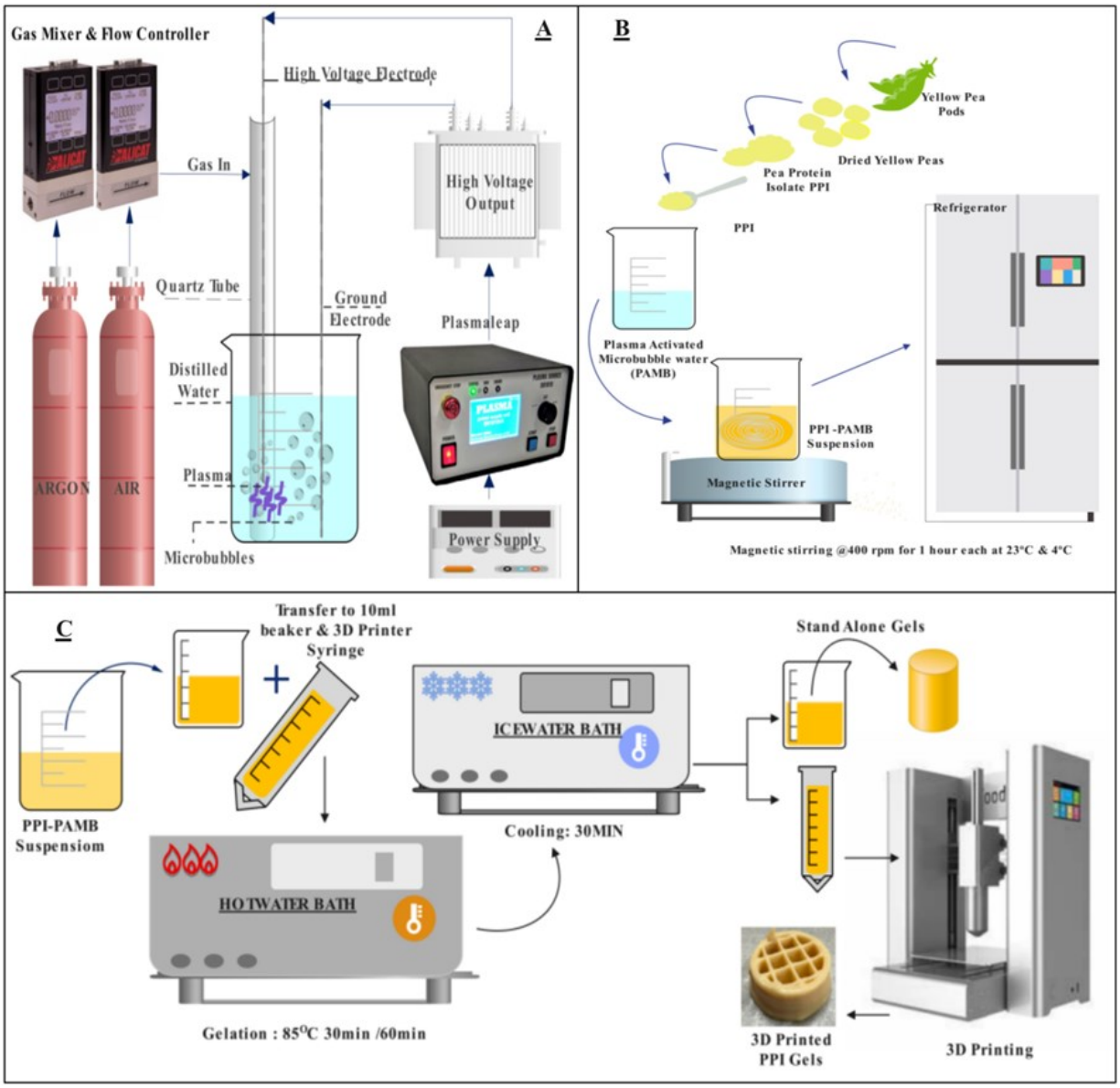

Figure 3.1 Schematic representation of experimental setup.

(A) Preparation of plasma activated microbubble water, (B) Preparation of pea protein isolate-plasma activated microbubble water suspension (PPI-PAMB suspension), and (C) Preparation of PPI-PAMB gel inks for 3D printing.

The combinations of gases used were 100% argon, 100% air, 90% argon along with, 10% air, and 80% argon along with, 20% air, at a fixed flow rate of 1 SLPM. In each of the experiments, the gas mixture was passed through the bubble reactor for 3 min before the application of high voltage to ensure that the gas flow was uniform and stable. The temperature of PAMB after 30 min of treatment increased to 40°- 43°C (Fig 3.1a).

3.2.3 Characterization of PAMB water

Concentrations of Reactive Oxygen Species (ROS) and Reactive Nitrogen Species (RNS) in the plasma activated microbubble water were estimated using test kits (CHEMetrics, LLC, Midland, VA, USA) as per the procedure outlined in the test kits.

3.2.4 Preparation of pea protein isolate suspension

The prepared PAMB (80 g) was mixed with pea protein isolate (PPI, 20 g) to produce pea protein suspension (20 solid wt.%) with magnetic stirring within 2 min of PAMB preparation. Preliminary trials were conducted to decide on the protein concentration to be utilized in the study. The suspension was then stirred for 1 h (400 rpm) at room temperature (~23 °C), followed by 1 h stirring (400 rpm) at 4°C (Fig 1B). Depending upon the gas combinations used, each suspension was labelled as ARG100 (100% argon only), AIR100 (100% air only) ARG90 (90% argon + 10% air), and ARG80 (80% argon + 20% air). The control sample was prepared by mixing distilled water (80 g) with PPI (20 g) and the sample was labelled as DW. (Figure 3.1b)

3.2.5 Preparation of PPI gels

Stirred PPI suspension was transferred to a 35 ml 3D printer syringe, tapped to remove air bubbles, and incubated for 30 or 60 min in a hot water bath maintained at 80°C, 85°C and 90°C. After incubation at specific temperatures for selected times, the samples were transferred to an ice-water bath maintained at 1°C ± 0.5°C for cooling for 30 min. Then, the syringes were taken out of the ice water bath, closed with a rubber cork, and mounted into the barrel connected to the 3D Printer for immediate printing. For characterization studies, the same procedure of gelation was followed using a 10 ml glass beaker instead of a 35 ml 3D printer. Upon complete cooling after gelation, the beaker was inverted, and the PPI gels were removed. Gelation was visually determined by the stand-alone nature of the gels (Figure 3.1C). The formed gels were stored at 4°C for 12-16 h before characterisation. The gels from PPI suspension prepared using PAMB were referred to as PPI-PAMB gels throughout this thesis.

3.2.6 Rheological analysis of PPI gels

The rheological properties of the PPI gels were tested on a TA Discovery HR-3 rheometer (TA Instruments, New Castle, DE, USA). This rheometer was equipped with a parallel plate geometry with a diameter of 40 mm The gel sample was placed on the rheometer plate for the frequency and amplitude sweep test. An amplitude sweep was performed in the 0.01–1% shear strain range at a frequency of 1 Hz to determine the linear range. Frequency sweep was conducted on gels compressed to 90% of their original height. Frequency sweeps were performed to determine the storage modulus G"" , loss modulus G", loss angle tan δ, and complex viscosity at oscillation frequency from 0.1 to 100 rad/s by applying a constant strain of 0.5% at 23°C. All rheological measurements were performed within the identified linear viscoelastic region at a strain value of 0.5%.

During the oscillatory shear test, the rheometer measures the amplitude of the applied stress and the amplitude of the resulting strain at each angular frequency (ω). The complex modulus (G∗), which combines the elastic and viscous properties of the gel, can be calculated as the ratio of the stress amplitude to the strain amplitude at each frequency. The values of G' and G" at each angular frequency can then be extracted from this complex modulus data. The complex viscosity (η*) can be calculated as the ratio of the complex modulus and angular frequency.

3.2.7 Mechanical properties of PPI gels

An Instron 5967 universal testing machine (Instron Corp., Norwood, MA, USA) equipped with a 50 N load cell was employed in testing the mechanical properties of the PPI gels. Each sample with cylindrical geometry (20 mm diameter and 25 mm height; measured using a ruler) was compressed to 70% strain, with a deformation rate of 1 mm/min at room temperature. The tests were conducted in triplicate. The stress-strain curve was obtained using the testing machine software to calculate three parameters: a). Young's Modulus (which is determined by the tangent slope of the preliminary linear stress-strain response), b). Compressive Strength (which is the maximum compressive stress attained), and c). Compressive Strain at break (which is the compressive strain value at maximum strength)

3.2.8 3D printing of PPI gels

The FoodBot 3D-Printer (ShiyinTech, Hangzhou, China) was used for the 3D printing of PPI gels. Based on the principle of micro-extrusion, this 3D printer had an operating system that determines the entire printing process by controlling a motor-driven plunger and cartridge that extrudes the sample for printing. The user interface screen of the printer enables the control of the basic

operations, such as initiation and termination of 3D printing, network connections, selection of the 3D model, printing temperature, and position of the plunger and cartridge.

For 3D printing, a 3D cylinder model of 10 mm height and 40 mm diameter was designed using Tinkercad® (Autodesk Inc., San Francisco, CA, USA). The created 3D cylinder model was then loaded into Cura Software (Version 15.02.06, Ultimaker, Geldermalsen, Netherlands), which sliced the model.STL file into layers and generated a G-code that can be detected by the 3D printer to print the physical object. This G-code was introduced into the 3D printer by an external USB to facilitate the 3D printing of the cylinder model. The syringes containing the PPI gels were loaded into a temperature-controlled cartridge (20 to 23°C) and 3D printed in accordance with the following printing conditions: 1.2 mm nozzle diameter, 1 mm layer height, solid bottom layer with 100% infill density and other layers with 50% infill density, rectilinear infill pattern, 20 mm/s speed, and 100% flow rate. The printed 3D images were photographed from different angles immediately after the completion of 3D printing.

3.2.9 Evaluation of storage stability of 3D printed PPI gels

The vertical length and the diameter at the bottom of the 3D printed PPI gels were measured. The measurement was obtained using a ruler while placing the sample on the parchment paper on which it was printed. Measurements were taken at constant intervals, i.e., 0 (immediately after printing), 24, 48 and 72 h. The 3D printed gels were stored in airtight containers at ~4°C. The tests were conducted in triplicate.

3.2.10 Statistical analysis

All the experiments were conducted in triplicate, and the data were statistically analyzed using statistical software (SAS® University edition; Proc Glimmax; SAS studio 9.4) using ANOVA

with Tukey's test as post-hoc analysis to identify significant differences between each sample group ($P < 0.05$).

3.3 Results and discussion

3.3.1 Characterization of PAMB

The physicochemical characterization of PAMB water produced with different gas concentrations, including pH, oxidation-reduction potential (ORP), and reactive species, indicates the formation of reactive oxygen and nitrogen species (RONS) as described in Table 3.1.

The production of PAMB water is essentially by the transfer of RONS from plasma to distilled water through microbubbles. Some of the chemical reactions involved in the formation of RONS are detailed below:

$$O_2 + O \rightarrow O_3 \quad (1)$$

$$\cdot OH + O \rightarrow HO_2 + O_2 \quad (2)$$

$$HO\cdot + HO\cdot \rightarrow H_2O_2 \quad (3)$$

$$NO + \cdot OH \rightarrow NO_2 \quad (4)$$

$$NO_2 + \cdot OH \rightarrow NO_3 + H \quad (5)$$

Ozone, the strongest oxidizing agent and one of the long-lived ROS in plasma is generated in the gaseous phase (Eq 1) and dissolved in water. The feed gas mixture has a significant impact ($p<0.05$) on the concentration of ozone in PAMB water. For instance, the highest concentration of ozone (17±3 ppm) was observed when AIR100 and ARG90 were used as the feed gas. The lowest ozone concentration was observed when ARG100 and ARG80 were used.

Table 3.1 Physicochemical characterization of PAMB water.

PAMB Samples	Ozone (ppm)	Peroxide (ppm)	Nitrite (ppm)	Nitrate (ppm)	pH	ORP (mV)
AIR100	17.9±2.9[a]	18.7 ± 5.8[d]	4.71± 3.70[a]	300 ± 18 [a]	2.77 ± 0.01[a]	514 ± 9 [a]
ARG80	4.83 ± 1.30[b]	21.3 ± 1.2 [c]	1.13 ± 0.10[b]	257 ± 35 [b]	2.77 ± 0.02[a]	509 ± 6 [a]
ARG90	13.5 ± 4.2 [a]	33.9 ± 2.9 [b]	1.17 ±0.20[b]	161 ± 7[c]	2.83 ± 0.01[a]	472± 2[b]
ARG100	4.31 ± 2.40[cb]	74.0 ± 2.1 [a]	1.1 ± 0.0 [b]	67.0 ± 0.2 [d]	2.75 ± 0.01[a]	356 ± 16 [c]

PAMB is produced with different gas combinations as feed gas mixture, measured indirectly after production. Values are expressed as the mean ± standard deviation of three replicates. Alphabets a,b,c,d within the same column indicate values that are significantly different ($p<0.05$).

Hydrogen peroxide (H2O2) is another major long-lived ROS in plasma. The H2O2 is formed by combining •OH radicals, as indicated in the equation 3. Similar to the ozone species, the concentration of H2O2 also was significantly ($p<0.05$) influenced by the feed gas mixture, however, H2O2 concentration was the highest when ARG100 (74±2 ppm) was used. When other feed gas combinations with argon, such as ARG90 and ARG80 were used, the H2O2 concentrations decreased with a decrease in argon gas concentration. This observation was further substantiated by the lowest H2O2 concentration when AIR100 was used. These results indicate that the quantities of reactive species in plasma activated solutions depend upon the feed gases utilized for plasma generation. A similar result has been established by Zhang et al. (2023), who showed that the spectral features and contents of reactive species in plasma activated water varied depending on the feeding gases and treatment times.

The presence of nitrate and nitrite indicates the generation of RNS in the PAMB water, produced through the dissolution of nitric oxide in gaseous plasma discharge (Equation 4 and 5). The results of the characterization experiment indicate that nitrate concentration was significantly dependent ($p<0.05$) on the feed gas combination. The nitrate species concentration was the highest when AIR100 (300ppm) was used, and it decreased with an increase in argon concentration in the gas mixture. For instance, the nitrate concentration was 257 ppm when ARG80 was used, while it was 161 ppm when ARG90 was used. The lowest concentration of nitrate (68 ppm) in PAMB was observed when ARG100 was used. Nitrite concentration was independent ($p>0.55$) of the % of air, in the case of feed gases with argon and air combination.

The pH of PAMB water produced with different gas combinations were highly acidic, with no significant correlation with the gas combination. The ORP of PAMB waters were considerably different, with PAMB prepared using AIR100 and ARG80 exhibited the highest ORP of 514± 9 and 509 ± 6 mV, respectively. The ORP was considerably low for ARG90 (472 ± 2 mV) and was the lowest for ARG100 (356 ±16 mV).

The characterization results indicate that the RONS concentrations in PAMB were the highest when AIR100 was used as the feed gas except for H2O2. The H2O2 concentration was the highest when ARG100 was used as the feed gas. It can be assumed that when argon is utilized as the feed gas, there may be a substantial increase in the generation of ·OH species, due to the dissociation of long-lived species (Zhang et al., 2023). This increased presence of the ·OH might be resulting in an increased quantity of hydrogen peroxide as the secondary species (Zhang et al., 2023)

The concentrations of RONS in PAMB were higher when ARG80 and ARG90 were used as the feed gases in comparison to when ARG100 was used. Since the structure and functional properties

of PPI are impacted by the concentration of RONS in PAMB (Bu et al., 2022a), it can be speculated that ARG80 and ARG90 would have a higher impact on gelation properties than ARG100.

3.3.2 Gelation of PPI prepared using PAMB

Preliminary trials were conducted to determine the most suitable concentration of PPI to facilitate gelation. Even though the minimum concentration required for heat-induced gel formation for PPI at near neutral pH was 16%, these gels were characterized by immediate deformation upon application of small force (O'Kane et al., 2005). A protein concentration of 18% was commonly used for gelation experiments, but even at this concentration, the PPI suspension did not form strong stand-alone gels. The PPI suspension prepared with distilled water at 20 wt%, produced a structure with gel-like properties; however, it did not hold shape and was not stable. The PPI suspension (20 wt.%) prepared with PAMB water treated AIR100 as the feed gas produced near-stand-alone gels when heated at 85°C for 30 min. With the increase in heating time to 60 min, the PPI gels formed were stand-alone gels, which did not deform even after applying a small force with a glass rod.

The gels prepared using PPI-PAMB were more stable and stronger when argon was used in combination with air as the feed gas for PAMB water production. With the feed gas combinations of 80% argon and 20% air, the PPI-PAMB gels formed were stand-alone gels, even after shorter heat gelation at 85°C for 30 min. When the heating time was increased to 60 min, stand-alone gels with better structure and stability were formed (Fig 2). Similar observations were made when the concentration of argon was further increased to 90 and 100%.

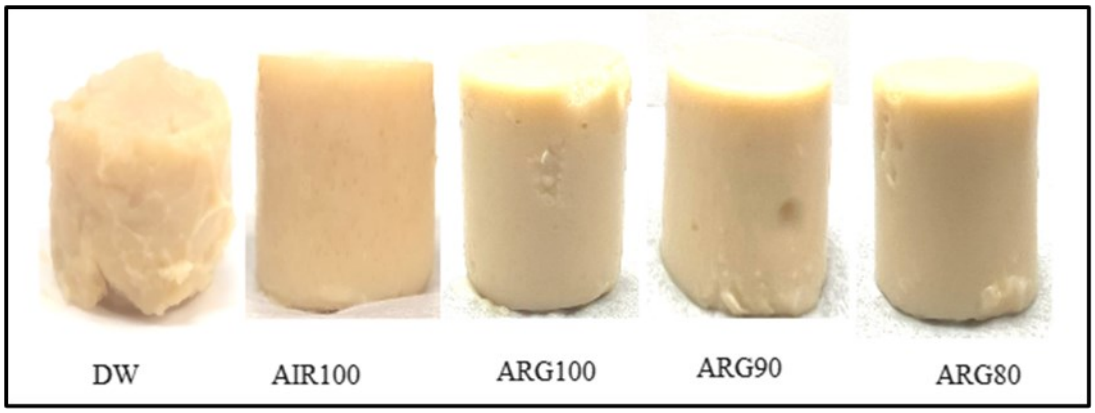

Figure 3.2 Images of PPI-PAMB gels.

Gels formed by heating at 85°C for 60 min, followed by cooling in ice water bath for 30 min. Images captured within 5 min of removal of gels from the glass beakers**.**

It can also be assumed that the low pH of the PAMB water might have influenced the gelation properties of pea protein. As indicated in Table 1, all the PAMB water samples were highly acidic, while DW was in a pH ~7.0, before the addition of PPI. In the case of PAMB water, the PPI suspensions were essentially prepared in an acidic medium, below the isoelectric point of pea protein. This probably led to a reduced solubility in the initial few minutes of agitation, indicating that there might have been some protein aggregation, due to the electrostatic protein-protein interactions. Upon continuous agitation, the solubility of PPI increased, leading to a homogeneous solution at the end of the stirring process. The final pH of all PPI suspension samples was near neutral at the end of 2 h stirring (6.75-6.9), with no statistical significance between samples. However, the PPI-PAMB suspensions had visibly higher viscosity than PPI-DW suspensions. Hence, it can be assumed that there was some initial protein aggregation in PPI suspension prepared from acidic PAMB water, which in turn would have positively impacted the gelation properties upon undergoing thermal gelation.

During thermal gelation, the weak non-covalent bonds such as hydrogen bonds and electrostatic interactions, are disrupted, causing protein denaturation, which in turn leads to the unfolding of protein chains and exposure of hydrophobic regions (Zhang et al.,2019). This would in turn lead to protein-protein interactions, such as hydrophobic and electrostatic interactions, which cause the formation of protein aggregates. A 3D network structure is formed with an increase in the number of protein aggregates. This structure of protein aggregates forms a gel-like network, trapping water and other components. This results in the retention of moisture and the formation of a gel structure (O'Kane et al., 2005). In this project, PAMB water consisting of RONS and other reactive species was used to dissolve PPI. During the heating of PPI solutions, the protein chains were unfolded, exposing more active side chains/groups. The long-lived reactive species in PAMB could react with these groups or side chains during heating, leading to more interactions to support gel formation compared to PPI solutions prepared using distilled water. Hence, the PPI solutions prepared by PAMB could form stronger gels.

Direct application of ACP treatment resulted in a marked improvement in the gelation properties of pea protein (Zhang et al., 2019). With the ACP treatment, the tertiary structure of pea protein is partially unfolded. Reactive oxygen species and reactive nitrogen species generated by the ACP cause oxidation of the unfolded protein, increasing the number of exposed free sulfhydryl groups and disulfide bonds. The gel network formed by pea protein during cold plasma treatment is stabilized by hydrogen bonding, which is crucial for its stability (Zhang et al., 2021). Since ACP had such a marked effect on pea protein gelation, a similar improvement in gelation properties could be observed with the application of indirect cold plasma treatment through plasma activated water. Similar mechanisms including protein unfolding and hydrogen bond formation by the

interaction of water molecules with the exposed -SH groups could be the reasons behind a marked effect on the gelation of pea proteins when PAMB-PPI suspension was utilized.

This observation on the effect of plasma activated water on protein structure is also in corroboration with the study that indicated that the application of plasma activated water increased the aggregation, strength, and water-holding capacity of chicken myofibrillar protein, which otherwise exhibited poor gelation qualities (Qian et al., 2021). Treatments using PAMB and plasma activated water could be considered superior to direct plasma treatment when it comes to protein functionality improvement because direct plasma treatment could induce severe oxidation of protein molecules (Qian et al., 2021). Moreover, plasma activated water treatment could be more uniform, with better interactions between protein molecules and reactive species, avoiding excessive oxidation of proteins (Bermudez-Aguirre, 2019b).

3.3.3 Rheological properties of PPI Gels

The G' indicates the ability of the material to store energy elastically, while G" indicates the non-ideal part of the gel network, which is formed by dangling or free ends able to dissipate energy (Zhang et al., 2022). Essentially, G' or G" value represents the solid-like or liquid-like properties of a sample, respectively, and a comparison of both indicates the viscoelastic behavior of the sample. The tan δ is a measure of the ratio between the viscous and elastic properties of a material. In a perfectly elastic material, the value of δ is equal to zero and for perfectly viscous materials, the value of δ is equal to 90^{o}.

All the tested PPI gel samples displayed prominent G' > G" over the tested frequency range of 1 to 100 rad/s, parallel to each other, and mostly frequency independent at all time-temperature combinations, indicating a clear elastic behavior and strong gel-like properties (Fig 3). For the

samples which are heated at 85°C for 30 min, ARG80 had the highest G' and G" when used as the feed gas, closely followed by ARG90 and ARG100 (Fig 3.3a).

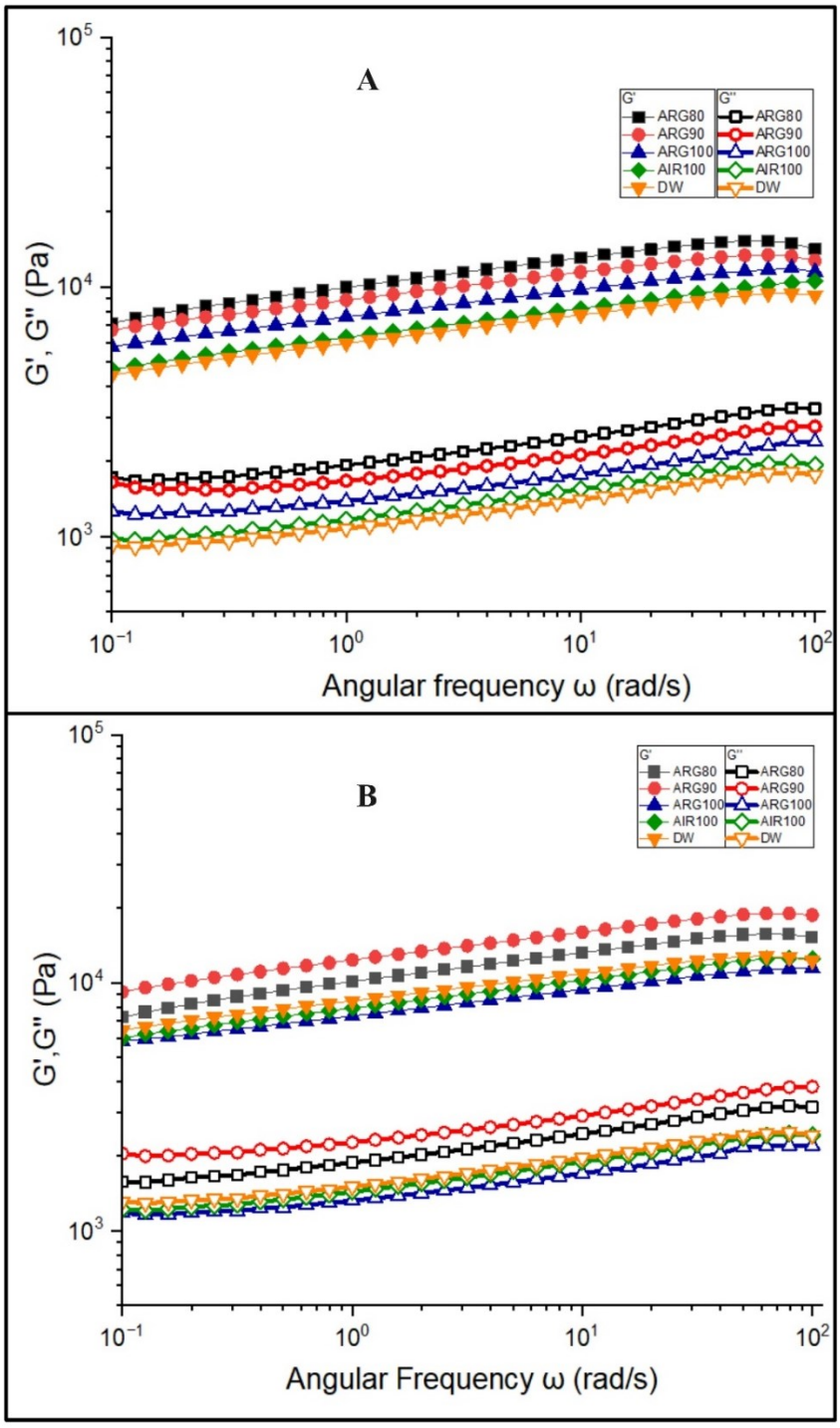

Figure 3.3 Frequency dependence of storage modulus (G') and loss modulus (G") of PPI-PAMB

Gels with different feed gas combinations when heating is done at 85°C for (A) 30 min and (B) 60 min, followed by cooling in an ice water bath for 30 min. The G' and G" values represent the storage and loss of energy in each deformation cycle, which reflects the elasticity (solid-like) and viscosity (liquid-like) properties of the sample, respectively.

A power law may be used to fit G' and G" with angular frequency (Moreno et al., 2020). The following equations can be applied.

$$G' = G_0' \cdot \omega^{n'} \quad (6)$$

$$G'' = G_0'' \cdot \omega^{n''} \quad (7)$$

G_0' and G_0'' are the storage and loss moduli at 1 rad/s, while n' and n" are exponents denoting the frequency dependence of G' and G". G_0' and G_0'' indicate gel rigidity or firmness i.e., the elastic and viscous resistance of the gels. A higher G_0' and G_0'' indicates higher gel rigidity and higher resistance to deformation. The power law parameters calculated from equations 6 and 7 are presented in Table 3.2.

Table 3.2 Power Law Parameters

Sample	G_0'	N_0'	G_0''	N_0''
ARG80-60MIN	10.08±0.08 ^{b}	0.109±0.003 ^{cb}	1.91±0.01 ^{b}	0.114±0.002 ^{ba}
ARG90-60MIN	12.42±0.08 ^{a}	0.104±0.002 ^{ed}	2.32±0.02 ^{a}	0.106±0.003 ^{d}
ARG100-60MIN	7.38±0.02 ^{e}	0.103±0.001 ^{ed}	1.35±0.01 ^{e}	0.108±0.003 ^{d}
AIR100-60MIN	7.91±0.03 ^{de}	0.109±0.001 ^{b}	1.46±0.01 ^{d}	0.117±0.002 ^{a}
DW-60MIN	8.47±0.06 ^{dc}	0.100±0.003 ^{ed}	1.54±0.01 ^{d}	0.109±0.002 ^{bc}
ARG80-30MIN	9.95±0.11 ^{b}	0.106±0.004 ^{ce}	1.98±0.01 ^{b}	0.110±0.002 ^{bc}
ARG90-30MIN	8.88±0.08 ^{c}	0.101±0.003 ^{e}	1.73±0.02 ^{c}	0.099±0.004 ^{e}
ARG100-30 MIN	7.58±0.04 ^{de}	0.105±0.002 ^{ce}	1.42±0.01 ^{e}	0.109±0.003 ^{bc}
AIR100- 30MIN	6.25±0.01 ^{f}	0.117±0.001 ^{a}	1.19±0.01 ^{e}	0.116±0.002 ^{a}
DW- 30 MIN	5.93±0.03 ^{f}	0.110±0.002 ^{cb}	1.1±0.01 ^{f}	0.112±0.002 ^{bc}

Values are expressed as the mean ± standard deviation of three replicates. Alphabets a,b,c,d,e,f within the same column indicate values that are significantly different ($p<0.05$).

ARG80 indicated significantly higher ($p<0.05$) G_0' and G_0'' values, when at the heating time of 30 min. The PPI gels prepared by AIR100 and DW samples heated for 30 min had low G_0' values, indicating the weakest gel behaviour. The G_0'' values of DW were also significantly lowest at the heating time of 30 min.

When the heating time was increased from 30 to 60 min, there was an overall increase in both G_0' and G_0'' values of all the PPI gels, indicating that gel rigidity or firmness increased (Table 2 and Fig 3B). In the case of samples heated for 60 min, ARG90 exhibited significantly higher G_0' and G_0'' values, indicating that the rigidity or firmness of ARG90 gels increased more than those of ARG80. In the case of ARG80 heated for 60 min, the G_0' and G_0'' values remained statistically similar to those heated at 30 min, indicating that heating time has no impact on the G_0' and G_0'' values for ARG80. A similar observation is seen in the case of ARG100 samples, wherein there is no significant impact of heating time in the values of G_0' and G_0''. The G_0' and G_0'' values of DW gels heated for 60 min are significantly lower than the corresponding values of ARG80 gels heated for 30 min, indicating that ARG80 samples have attained a higher gel strength and viscoelastic properties than DW samples, in half the heating time.

It can also be observed that feed gas combinations that include a mixture of argon and air heated at 30 min (ARG90 and ARG80) induce stronger gels with higher G_0' and G_0'' values when compared to the feed gases of 100% argon and 100% air (ARG100 and AIR100) heated at 60 min. This indicates that even within PAMB feed gases, there are some intrinsic factors related to specific reactive species generated by certain gases affecting the viscoelastic properties of PPI gels.

The n' and n'' exponents corresponding to G_0' and G_0'' showed differences, but without any statistical significance, other than AIR100-60 min (Table 2). However, for all samples, $n' < n''$,

indicating that the rate of decrease of G′ was lower than the rate of decrease in G″ with a decrease in angular frequency (ω)

Along with RONS, some reactive argon species might also be contributing to this gelation effect in pea proteins. Bu et al. (2022b) have reported that all reactive species generated as an outcome of cold plasma can induce protein denaturation and form disulfide-linked soluble aggregates, thereby resulting in better gelation properties in pea proteins. Hence, more experiments regarding the quantification of reactive argon species need to be further conducted to clearly understand its role in gelation.

The tan δ values of all PPI gels were observed to be in the range of 0.1-0.3 at all frequencies (Fig 4), indicating the prominent elastic behaviour of all the samples. Complex viscosity describes the overall resistance to flow exhibited by a viscoelastic material, taking into account both the elastic and viscous components. All samples showed a marked decrease in complex viscosity with an increase in frequency, which is an indication of shear thinning behavior corresponding to non-Newtonian fluids. Shear thinning is attributed to the elongation or stretching of molecules with an increase in shear, causing a decrease in molecular entanglements, which in turn enables the sliding between molecules, thereby decreasing the viscosity (Picout and Ross-Murphy, 2003). The complex viscosity of the gels is noted to be higher when PAMB water with argon feed gas was used for gelation, in comparison to distilled water. ARG100 had higher complex viscosity than DW and AIR100. When a combination of air and argon was used, the complex viscosity further increased, with ARG80 showing a higher complex viscosity than ARG90.

These results indicate that the type of feed gas utilized for PAMB generation may have an impact on the denaturation temperature of proteins as well as the rheological properties of PPI gels. Since the type of feed gas directly determines the nature of reactive species in PAMB, it can be assumed

that various reactive species in each PAMB water are inducing specific rheological properties. This conclusion is also supported by the finding of Bu et al. (2022), who have reported that reactive species, such as O_3, NO_x, H_2O_2 and OH generated in ACP with air as feed gas can induce enhanced protein solubility and increase in soluble aggregates. The authors also noted that the balance between hydrophobicity and surface charges facilitated protein-protein and protein-water interaction, leading to the formation of strong PPI gels

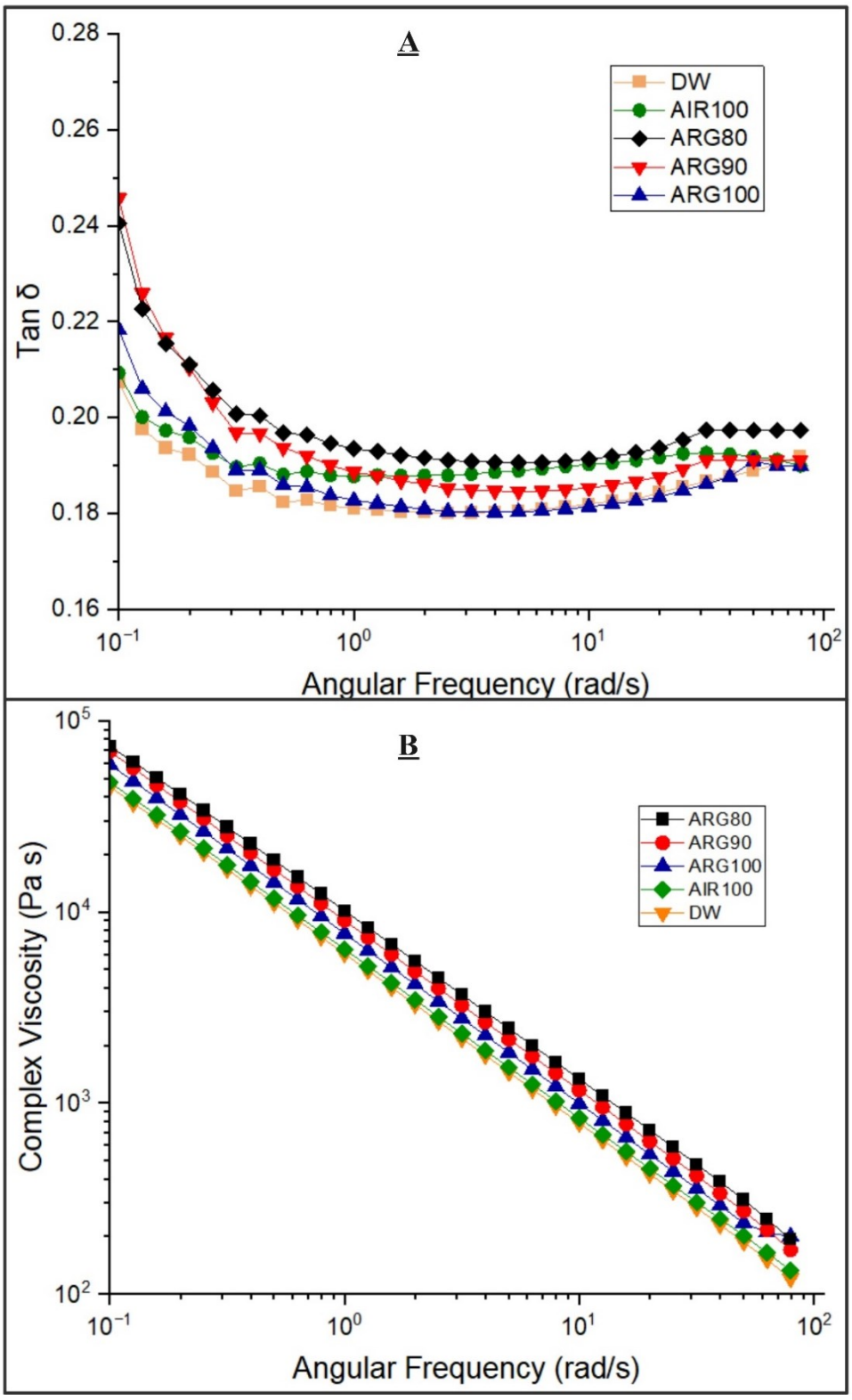

Figure 3.4 Frequency dependence of (A) tan δ and (B) complex viscosity of PPI gels.

Gels with different feed gas combinations when heating is done at 85°C for 60 min followed by cooling in an ice water bath for 30 min.

Regarding the effect of temperature on G' and G'' of PPI gels (Fig 3.5), there was an increase in G' and G'' with an increase in temperature from 80 to 90°C with 60 min heating, indicating that a stronger gel was formed with an increase in heating temperature. As the heating temperature was increased, the protein molecules unfolded to a greater extent. This resulted in an increase in the number of active groups that were exposed, making it easier for covalent and non-covalent interactions to take place. The interactions formed stronger three-dimensional gel networks. Similar results of increase in viscoelastic properties with increase in heating temperature were reported by Zhang et al. (2021).

Among the PPI gels, DW gels showed the least increase in G' and G'' values with an increase in temperature, at all tested frequencies. In the case of AIR100, at all tested frequencies, both G' and G'' values increased considerably with an increase in temperature from 80 to 85°C (15 kPa to 20 kPa) however from 85 to 90°C, the extent of increase was lesser (e.g., 20 kPa to 22 kPa). In the case of ARG80, there was a considerable increase of G' and G'' values when temperature increased from 80 to 85°C (15 kPa to 22 kPa); however, with further increase of temperature to 90°C, there was a very slight increase in gel strength. The increase in viscoelastic properties with increase in temperature can be attributed to a greater degree of protein unfolding with the application of higher temperature for heating. It can also be assumed that in case of ARG80 and ARG90, complete protein denaturation might have occurred at around 85°C, explaining why there is no increase in viscoelastic properties even when temperature was increased to 90°C. These results indicate that the type of feed gas utilized for PAMB generation may have an impact on the denaturation temperature of proteins as well as the rheological properties of PPI gels. Since the

type of feed gas directly determines the nature of reactive species in PAMB, it can be assumed that various reactive species in each PAMB water are inducing specific rheological properties.

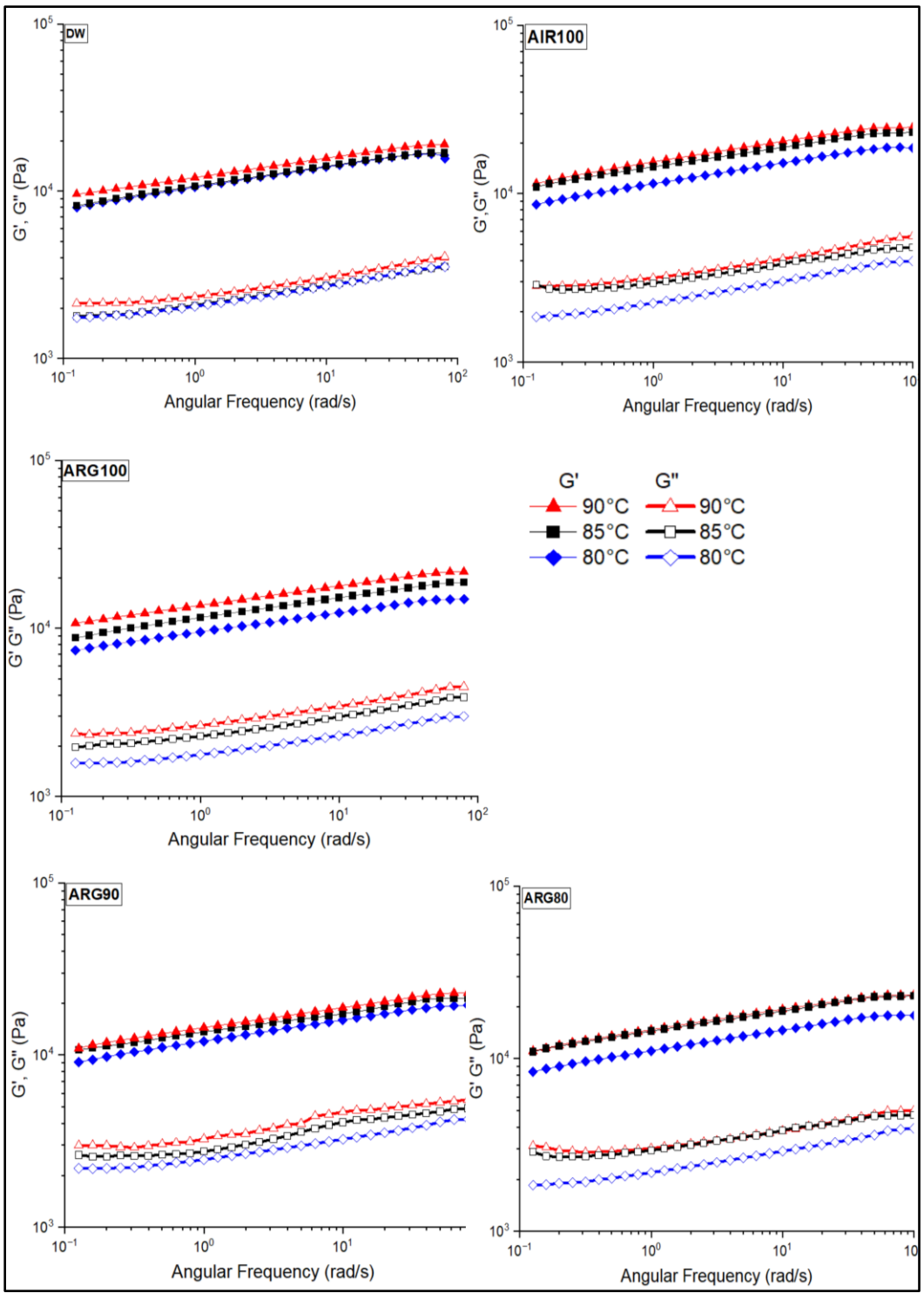

Figure 3.5 Frequency dependence of storage modulus (G') and loss modulus (G") of PPI-PAMB at 80°C, 85°C and 90°C

Gels were formed by heating at different temperatures (80°C, 85°C, 90°C) for 60 min, followed by cooling in an ice water bath for 30 min.

This conclusion is also supported by the finding of Bu et al. (2022), who have reported that reactive species, such as O_3, NO_x, H_2O_2 and OH generated in ACP with air as feed gas can induce enhanced protein solubility and increase in soluble aggregates. The authors also noted that the balance between hydrophobicity and surface charges facilitated protein-protein and protein-water interaction, leading to the formation of strong PPI gels.

When analyzing the PAMB gels, it was determined that ARG90 and ARG80 exhibited superior viscoelastic properties compared to both ARG100 and AIR100. This indicates that PAMB produced with a combination of gases (air or argon) in the feed mixture had better gelling properties than PAMB produced by either of these individual gases. This phenomenon may be explained in connection with the results of RONS characterization, wherein AIR100 and ARG100 had either the highest or lowest RONS quantities. AIR100 had significantly high amounts of ozone, nitrite, and nitrate but significantly low quantities of H_2O_2. In contrast, ARG100 had a significantly high amount of H2O2 but very low quantities of ozone and nitrate. At the same time, ARG80 and ARG90 had considerable quantities of ozone, H_2O_2, and nitrates, indicating the presence of both ROS as well as RNS. It may be assumed that the presence of both ROS and RNS led to the increase in viscoelastic properties of PPI gels prepared by PAMB water with ARG90 and ARG80 as feed gases. A similar conclusion was reached by Bu et al. (2022), where the authors established that O_3 and OH reactive species were significant in improving the functional properties of PPI. In addition, there may be contributions from reactive Ar species and other reactive oxygen species (OH radicals, superoxide anions, and singlet oxygen, which were not determined in this study) on improving the viscoelastic properties of PPI gels, which need further research.

3.3.4 Mechanical properties of PPI Gels

The compressive strength, compressive strain at break, and Young's modulus of PPI gels prepared by heat gelation at 85°C for 30 and 60 min are presented in Table 3.3. These properties were used to gain insights regarding the textural and structural properties of the 3D printed PPI gels. The higher the compressive strength, the better the potential gel stability and resistance to failure once printed, especially as the printed object becomes taller in height. Conversely, the higher the compressive strain at break, the more resistant the gel is to fracture. Overall, all gels exhibited an initial stiffening followed by a linear stress-strain response up to maximum stress (and strain at break). The compressive failure was ductile in nature with a slow drop in stress with increasing applied deformation. This latter behaviour was important to ensure good printability of the 3D printed gels (i.e., extrusion without line breakage).

The feed gas composition and heating time had a significant impact ($p<0.05$) on the compressive strength of the PPI gels. After 30 min of heating, compressive strength values of all PPI-PAMB gels except AIR100 gels were significantly different from those of DW gels. After 60 min heating, DW gels had significantly lower compressive strength compared to all PPI-PAMB gels. All PPI-PAMB gels did not exhibit any significant difference in compressive strength values among each other. It can also be noted that DW gels did not display a statistically significant increase in compressive strength with an increase in heating time from 30 to 60 min (Table 3).

Table 3.3 Mechanical properties of PPI gels (Compressive strength, compressive strain, and young's modulus) gelated at 85°C for 30 and 60 min, respectively. The data is compared within each column.

Heating time	PPI gels	Compressive strength (kPa)	Compressive strain (mm/mm)	Young's modulus kPa
30MIN	DW	2.55 ± 0.61 ^{d}	0.18 ± 0.01 ^{d}	16.4 ± 3.0 ^{c}
	AIR100	2.72 ± 0.08 ^{d}	0.19 ± 0.00 ^{cd}	21.9 ± 1.0 ^{bac}
	ARG80	3.83 ± 0.61 ^{bc}	0.23 ± 0.01^{cb}	21.2± 2.2 ^{bac}
	ARG90	4.40 ± 0.20 ^{dc}	0.21 ± 0.02^{cbd}	17.3 ± 3.8 ^{c}
	ARG100	3.81± 0.21 ^{dc}	0.20 ±0.03^{cd}	22.1± 1 ^{bac}
60MIN	DW	2.57 ± 0.44 ^{d}	0.21 ± 0.01 ^{cbd}	18.1 ± 5.9 ^{bc}
	AIR100	3.94 ± 0.40 ^{bac}	0.22 ± 0.03 ^{cb}	21.0 ± 1.1 ^{ba}
	ARG80	4.03 ± 0.81 ^{bac}	0.28 ± 0.03 ^{a}	21.6 ± 3.0 ^{bac}
	ARG90	4.76 ± 0. 88 ^{a}	0.24 ± 0.02 ^{b}	24.9 ± 5.6 ^{a}
	ARG100	4.49 ±0.55 ^{ba}	0.22 ± 0.02 ^{cb}	24.3± 4.1 ^{bac}

Values are expressed as the mean ± standard deviation of three replicates. Alphabets a,b,c,d within the same column indicate values that are significantly different ($p<0.05$).

In the case of PPI-PAMB gels, ARG100, AIR100 and ARG90 displayed a statistically significant increase in compressive strength with an increase in heating time from 30 to 60 min, however, the compressive strength of ARG80 remains statistically similar even with the increase in heating time from 30 to 60 min.

Upon estimating the effect of heating temperatures (80, 85, and 90°C) for 60 min for different PPI gels, the increase in heating temperature from 80 to 85°C showed a significant impact on the compressive strength of PPI gels (Appendix 1). However, with the increase in heating temperature from 85 to 90°C, there was no significant impact on the compressive strength. The ARG90 gels heated at 90°C for 60 min formed the gels with the highest compressive strength (Appendix 1), followed by ARG90 gels heated at 85°C for 60 min. Compressive strength, which points toward

the gel strength during compression, is an important factor that determines the structural stability of the 3D printed gels (Li et al., 2021). These results can also be correlated with the 3D printability of PPI gels.

Heating time increase from 30 to 60 min also had a significant impact ($p<0.05$) on the compressive strain at break of PPI gels heated at 85°C, depending on the feed gas used. Similar to the results in compressive strength, a heating time of 30 min did not result in significantly different compressive strain at break values among PPI-PAMB gels, while the compressive strain at break values were different from DW gels. With an increase in heating time to 60 min, ARG80 had a significant increase in compressive strain at break, while all other PPI gels remained statistically similar. The effect of heat gelation temperatures (80, 85, and 90°C) on the compressive strain of PPI gels for 60 min indicates similar results to that of compressive strength (Appendix 1). ARG80 PPI gels heated at 85°C had the highest compressive strain among all the samples, followed by ARG90 heated at 90°C. PPI-DW samples heated at all temperatures had lower compressive strain values than PPI-PAMB gels (Appendix 1). However, the compressive strain value of only ARG80 gel was statistically different compared to that of DW gel. A higher compressive strain at break of a food gel provides an indication of toughness of the material and its suitability for 3D printing and has been found to correspond to better extrudability and layer adhesion in 3D food printing (Liu et al., 2018). With a higher compressive strain at break, it can be assumed that ARG80 gels heated for 60 min would exhibit properties favourable for extrusion 3D printing.

Young's modulus is the resistance of deformation of gels due to the applied load and, regarding 3D printing, it indicates the stiffness of the 3D printed product. Young's modulus of the PPI-PAMB gels was found to have no significant impact with an increase in heating time or feed gas composition. The overall results of compressive strength and compressive strain at break of PPI-

gels indicate that the heating time of 60 min results in gels with better properties. After 60 min of heating time, all PPI-PAMB gels have higher compressive strengths than DW and ARG80 had the highest compressive strain at break.

3.3.5 3D printability of PPI Gels

Figure 3.6 presents the 3D printed PPI gels made from PAMB water, heated at 85°C for 30 and 60 min. The native pea protein suspensions were not readily extrudable however, gelation improved the printability of pea protein isolates. Even though all PPI gels could be extruded from the nozzle of the 3D printer, the printing quality varied widely within the samples.

The heat gelation time of 30 min at 85°C followed by cooling for 30 min considerably improved the extrudability of the PPI. Even though the DW gels produced at this condition were easily extruded from the 3D printer, an overall structural instability could be observed, causing the 3D printed shapes to easily cave in and deform. Typical creep behaviour of viscoelastic materials, indicating a gradual and time-dependent deformation under a constant applied load, can be observed in the first layer of the extruded PPI gel, causing it to deform and spread immediately upon printing. With more layers depositing on top of each other, the creep of the first layer leads to the distortion of the entire product, causing the 3D printed cylinder to sag and cave in due to gravity loading. A distinct lack of adhesion between layers also can be observed here.

When DW was replaced with PAMB water to prepare PPI gels, there was a notable improvement in printability, with the 3D printed gels holding their structure and shape with minimal deformation. It can be noted that there was no caving-in of the top layer, indicating that the top layers remained adhered to the bottom layers. Even though AIR100-30 min and ARG100-30 min samples showed marked improvement in printability and structural strength, the creep behaviour

was still observed in bottom layers, as it tends to spread out over time. It was to be noted that as in the case of DW, the creep behaviour of the gel did not lead to total deformation of the sample, as the layers deposited on top of the bottom layer tend to hold shape. It can also be assumed that the layers other than the bottom-most layer did not exhibit creep behaviour. A possible reason would be the surface tension acting on each layer to keep them intact. In the case of the bottom-most layer, the observed time dependent spreading (creep) may be due to the increasing weight of subsequent layers coupled with a smooth bottom surface (i.e., deposition on parchment paper). For all other subsequent layers printed on top of the bottom layer, the surface tension of each layer provides resistance to creep behaviour. It is postulated that a print bed with a rougher surface or cooling capabilities may prevent the first layer from spreading. Similar spreading of the first layer has also been observed in other studies (Lim et al., 2023).In the case of ARG80-30 min and ARG90-30 min, the printability was improved, with decreased creep behaviour of the bottom layers, enabling accurate layer deposition. A slight layer-on-layer adhesion was observed, with printed lines of the final product visible and displaying the layer-over-layer stacking properties distinctively. Moreover, the bottom layers of the gels held the shape and did not spread out as the height of the printed shape increased, indicating minimal creep behaviour in these samples.

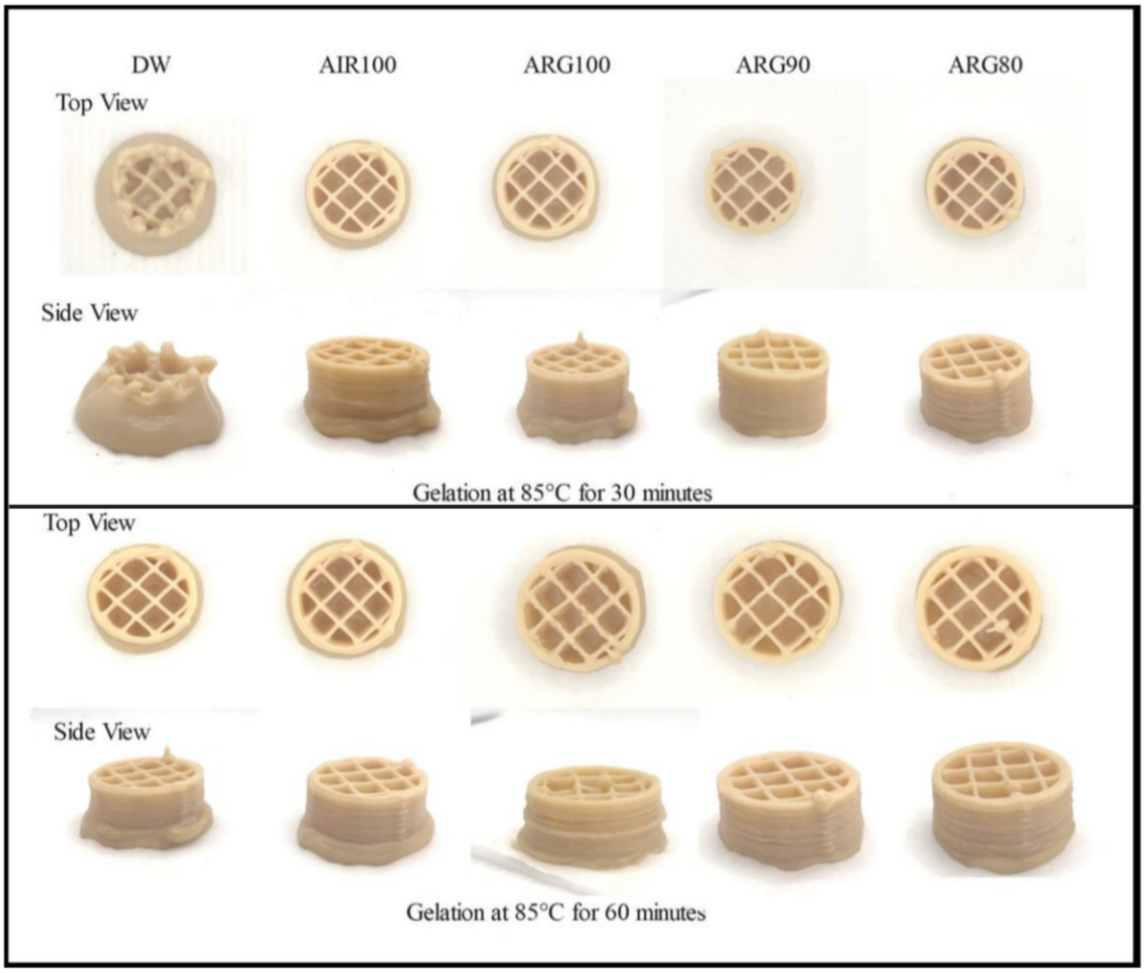

Figure 3.6 Images of 3D printed PPI gels.

PPI Gels gelled at 85°C for 30 and 60 min respectively, followed by cooling in ice water bath for 30 minutes. Images captured within 5 min after completion of 3D printing.

With the increase of gelation time to 60 min, an ability to resist the deformation was observed in DW gels. However, the structural stability of 3D printed DW gels was poor, with a display of creep behaviour. The base and bottom layers were deformed and spread out, while the top layers led the structure without deformation. A similar creep behaviour is seen in the bottom layers of AIR100, with the top layers holding the structure. In the case of ARG100, the creep behaviour of the bottom layer was observed as minimal, however, the layer-over-layer deposition was not uniform, indicating a lack of adhesion between layers.

ARG80 and ARG90 gels heated for 60 min displayed better printability, with smooth extrusion from the nozzle, clearly visible printed lines, and layer-over-layer stacking properties. It was to be noted that the creep behavior of the bottom layers was the least in these gels in comparison to all other printed gels. These ARG80 and ARG90 gels exhibited better shape retention and structural stability, in comparison to all other gels.

The printability of a food ink is characterized by its ability to adapt to printing processes and deposition without compromising the structural integrity (Jiang et al., 2022). The extrudability, printability and structural strength of 3D printed PPI gels could be correlated to the gelation of pea protein isolates, rheological, and mechanical properties of PPI gels and hence the specific reactive species concentrations in PAMB water. The G' or G" values of PPI-PAMB gels at both 30- and 60-min gelation time indicated the elastic nature, which was probably the reason why the PPI-gels were extruded smoothly from the nozzle (Lipton, 2017). The highest G_0' & G_0'' values were calculated for ARG90 gels, followed by ARG80 gels, heated for 60 min and these samples displayed the best 3D printability. This explains why the creep behaviour was less on ARG90 and ARG80 samples, as a higher G_0'' value corresponds to a lower creep behaviour, indicating that the material resists deformation. (Kim et al., 2018; Kim et al., 2021; Outrequin et al. 2023)

All PPI-PAMB gels at 60 min heating had higher compressive strengths than DW gels, while ARG80-60 min was the most ductile, as indicated by higher compressive strain at break values. Another notable observation was the correlation of concentrations of RONS in PAMB water with the printability of PPI-PAMB gels. The characterization results indicate that both ARG80 and ARG90 had ROS and RONS values ranging between those for ARG100 and AIR100. Regarding the printability of PPI-PAMB gels, it may be speculated that the presence of both ROS and RNS is required for the best printing properties in PPI gels.

3.3.6 Storage stability of 3D printed gels

The storage stability of 3D printed PPI gels after 24 and 72 h is illustrated in Figure 3.7 and Figure 3.8 respectively. The results indicate that 3D printed PPI gels prepared using ARG90 and ARG80 resisted deformation (change in length and diameter) after 24 h post-printing storage, with minimal deformation even after 72 h of storage. The 3D printed gels prepared using DW exhibited significant deformation within 24 h after printing, with the entire structure caved in at the top by the end of 72 h storage. The dimensions of 3D printed PPI gels prepared using ARG90 and ARG80 were comparable to that of a fresh 3D printed gel even after 24 h of storage. For these 3D printed gels during 48 and 72 h storage, there was only a very slight variation in dimension in comparison to DW gels.

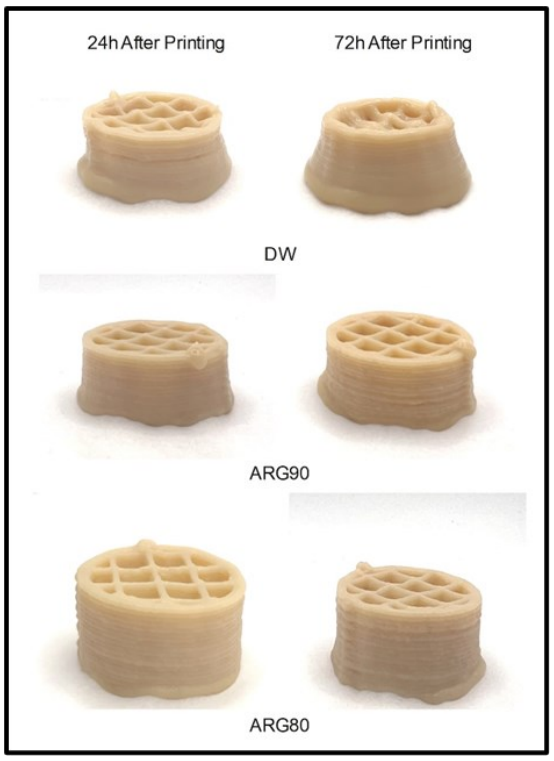

Figure 3.7 Storage deformation images of 3D printed PPI gels.

PPI gels gelled at temperature of 85°C for 60 min, followed by cooling at 4C for 30 min. Images taken upon storage for 24 and 72 h, respectively.

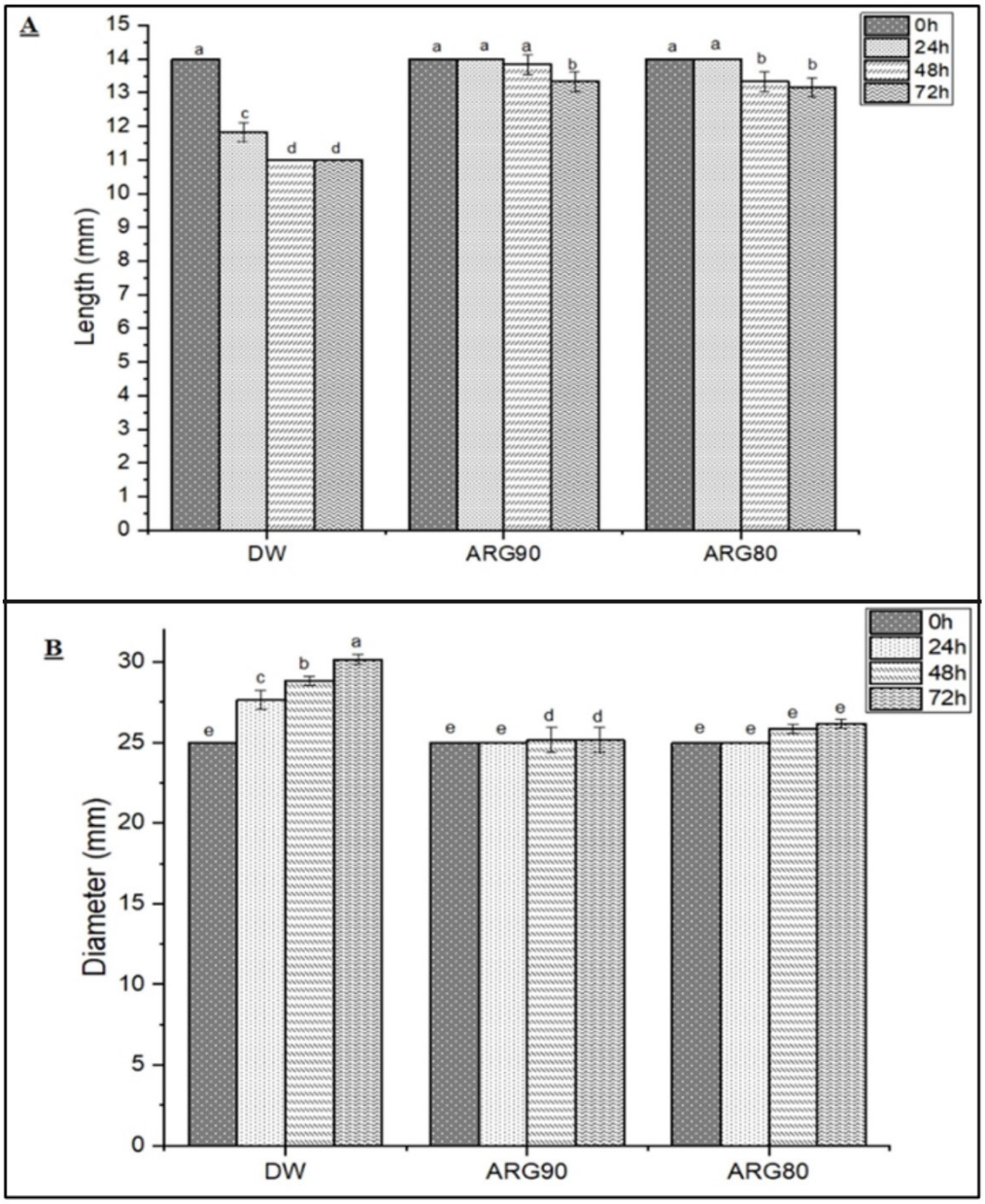

Figure 3.8 Change in dimensions of 3D printed PPI gels upon storage.

(A) length and (B) diameter of 3D printed PPI-DW and PPI-PAMB gels upon storage up to 72 h.

The storage stability of PPI-PAMB gels can also be attributed to the better creep resistance of ARG90 & ARG80. For the DW gels, significant creep behaviour over time was observed which correlated with the lowest G_0" of all conditions tested. In the case of ARG90 and ARG80 samples,

a higher G_0" likely resulted in lower creep behavior, characterized by low deformation over time due to gravitational forces.

The results of this storage study demonstrate that 3D printed PPI gels prepared using PAMB had a higher structural stability and resistance to deformation upon storage. This indicates the feasibility of cold plasma application for improving the structural stability and functionality of PPI gels.

3.4 Conclusions

In this study, pea protein isolate (PPI), a natively non-extrudable food ingredient, which is generally unsuitable for 3D printing achieved better 3D printing properties by the application of plasma activated microbubble (PAMB) water and thermal gelation methods**.** The rheological and mechanical properties indicate that PPI suspension prepared using PAMB, followed by gelation at a heating temperature of 85°C for 60 min, and cooling at 4°C for 30 min; resulted in the best 3D printability. The PAMB water generated using a mixture of 80% argon and 20% air (ARG80) as well as 90% argon and 10% air (ARG90) was used to prepare 3D printed PPI gels with greater structural stability. The improved structural stability of these 3D-printed PPI gels was possibly due to the enhanced rheological and mechanical properties, which could be related to the optimal reactive oxygen and nitrogen species concentration in PAMB prepared using ARG80 and ARG90. The ideal gelation, gel strength, and 3D printability of 3D printed gels may correspond to the presence of both ROS and RNS, rather than either one. Overall, this study showed the application of PAMB in improving the structural properties of PPI and its 3D printability; however, further studies are required to estimate the effect of specific reactive species, especially the contribution of reactive argon species that might have contributed to the functionality and improved printability of PPI gels.

Chapter 4 Freeze drying of 3D printed pea protein gels

4.1 Introduction

3D-printed foods such as chocolate can be considered ready-to-consum, immediately after printing. However, several other food products that undergo 3D food printing require several additional post-printing steps before being deemed fit for consumption (Dankar et al., 2018). Traditional food processing techniques, such as cooking in the forms of baking, boiling, or frying, can be utilized as post-printing techniques, but this would essentially include an array of altered textural properties and physical modifications that may or may not be agreeable with the final desired product quality. Moreover, traditional cooking can also lead to chemical changes such as protein denaturation, water loss, evaporation, and changes in color, volume, and nutritional value (Sun et al., 2018).

Freeze drying, or lyophilization, is a preservation technique that removes moisture from frozen foods, subjecting them to low temperature and pressure conditions. This process essentially involves freezing the food item and placing it in a vacuum, where the ice crystals evaporate by sublimation (Nowak and Jakubczyk, 2020). Freeze drying of foods is a popular food preservation process in the food industry due to its ability to preserve the texture, flavor, and nutritional value while extending its shelf life. Upon comparison between the two post-3D printing techniques, i.e., oven drying and freeze drying, to understand the ability to preserve shape stability and texture, it was established that freeze drying retained the 3D printed structure better than the oven drying process. With an increased hardness and dry matter content, freeze dried food had a solid structure, unlike its dried counterpart (Dankar et al., 2018).

Furthermore, freeze drying is ideal for preserving sensitive or delicate foods, such as fruits and vegetables, as it avoids the damage caused by heat treatments like canning or dehydration (Majumdar, 2007). Studies on freeze drying of fruits such as oranges (Silva-Espinoza et al., 2020), blueberries (Munzenmayer et al., 2020), blackberries (Franceschinis et al., 2014), guava, papaya (Hawlader et al., 2006), and strawberries (Meda and Ratti, 2005) as well as vegetables such as carrot (Regier et al., 2005), pumpkin, (Ciurzyńska et al., 2014), (Guiné and Barroca, 2012) peppers (Guiné and Barroca, 2012) and asparagus (Nindo et al., 2003) have been conducted for the last two decades. Even though freeze drying can induce some textural and mechanical property alterations, it has been proven to be a far superior drying technique to conventional oven drying or spray drying (Bhatta et al., 2020). This significant observation has led to the application of freeze drying to non-traditional food sources in the last few years.

Food products such as soy protein isolate/κ-carrageenan hydrogels (Yang et al., 2022), whey protein hydrogels (Manzocco et al., 2021), chickpea protein isolates (Kaur and Singh, 2007) and quince seed gum (Ahmadzadeh-Hashemi et al., 2023) have been studied for freeze drying. Similarly, pea protein isolates have also been investigated for freeze and spray drying on the interface and foam stabilizing properties (Yang et al., 2022). A study involving the drying of 3D-printed pumpkin snacks found that freeze drying resulted in increase on the crispness and crunchiness of the snack, thereby increasing its sensory acceptance (Chen et al., 2022). Another study, which involved encapsulation of probiotics using a combination of 3D printing and freeze drying, noted that the 3D printed products transformed a semi-solid to a solid-like state after freeze drying, as confirmed by increased hardness and decreased water activity, demonstrating a potential to produce shelf-stable supplement food (Kuo et al., 2022). However,

no studies investigated the properties associated with freeze dried pea protein gels. Since freeze dried pea protein isolates have the potential to be utilized as encapsulation agents or protein-rich breakfast cereals, it is crucial to understand the physical and thermal properties associated with freeze dried PPI gels.

This study is an extension of the work conducted in Chapter 3 and aims to investigate the effect of a post-processing treatment, such as freeze drying, on 3D printed PPI gels made out of PAMB water. Considering that it has already been established that PAMB-PPI gels have better gelation, mechanical properties, and 3D printability in comparison to DW-PPI gels, it is essential to understand any differences in textural and structural properties of 3D printed PPI gels prepared from different methods. The study investigated the applicability of freeze drying as a potential post-processing treatment for 3D printed PPI gels.

4.2 Methods and materials

4.2.1 Preparation of 3D printed PPI gels

The 3D Printed PPI gels were prepared using the PPI-PAMB suspension gelated at heating temperature of 85°C for 60 min, followed by cooling at 4°C for 30 min, as described in Chapter 3. In this study, PAMB feed gas combination of only ARG80 (80% argon and 20% air) and ARG90 (90% argon and 10% air) were utilized, as these two PAMB combinations resulted in the most structurally stable 3D printed gels. PPI-DW suspension gelated at same time-temperature was used as the control samples. The 3D printed PPI gels prepared using distilled water and gelated at a heating temperature of 85°C for 60 min, followed by cooling at 4°C for 30 min, were set as the control sample. The samples were labeled ARG80, ARG90, and DW throughout the experiment.

All parameters associated with PAMB preparation, gelation, and 3D printing was followed as detailed in Chapter 3.

4.2.2 Freeze drying of 3D printed PPI gels

The 3D printed PPI gels were transferred to airtight containers immediately after 3D printing and stored in a deep freezer at a temperature range of -20° to -25° C for 24 h to ensure complete freezing of the samples. The frozen PPI samples were then lyophilized using a cabinet freeze dryer at -50°C for 72 h at near vacuum. After the complete removal of moisture, the samples were put back into airtight containers and stored below -20°C in a deep freezer until further characterization.

4.2.3 Moisture content and water activity of freeze dried PPI gels

The freeze dried PPI samples were ground to a fine powder using a coffee grinder to test the moisture content and water activity. The moisture content was measured using the oven-drying method; 1.5 g of finely ground freeze dried PPI powder was taken in an aluminum pan and heated at 105 ± 1 °C for 8 h in a hot air oven to obtain constant weight loss. The water activity was measured using an AquaLab Water Activity Meter at ambient temperature (22 ± 1°C).

4.2.4 Textural properties

The freeze dried 3D printed PPI gels were characterized for texture profiling using a texture analyzer (TA. XT plus C, Texture Technologies Corp. and Stable Micro System, Ltd. Hamilton, MA, USA). A compression test was used to estimate the external force required to compress the samples to 80% of their original height. A P/50 probe (diameter: 2 mm) was used to compress the sample, which was placed at a height of 20 mm. Standard Texture Profile Analysis (TPA) test conditions were used in all experiments, with a trigger force of 5 g, set at a target distance of 10

mm, 1.0 mm/s of pretest speed, and 5.0 mm/s test and post-test speed. The delay time between the first and second compression was 5 seconds.

Textural properties, such as hardness, fracturability, adhesiveness, chewiness, and cohesiveness were calculated using the instrument software. Hardness is the maximum force required to compress the sample and was calculated as the peak force recorded on the force-time curve of the compression test. Fracturability is the force required to fracture a sample and was determined as the point on force-time curve, where the force starts to decrease after the first peak. Adhesiveness is the stickiness of the sample and is calculated as the negative area under the force-time curve during the separation phase in compression. Cohesiveness is the ability of the sample to stick together during chewing and is calculated as the ratio of the positive force areas of the second compression and first compression in the force-time curve. Chewiness is a measure of the energy required to masticate the sample and is calculated as the product of hardness, cohesiveness and springiness.

4.2.5 Scanning electron microscopy (SEM)

The internal microstructure of freeze dried 3D printed PPI gels, freeze dried PPI gels, and freeze dried PPI suspensions were examined using scanning electron microscopy (SEM). The freeze dried samples were sliced into 0.5 mm thick pieces to observe the internal cross sections. The slices were carbon taped and sputter-coated with gold (Au) for 60 s, coating at 5-10 mA current, (Denton Desk II, New Jersey, USA) to avoid charging issues during the electron scanning. The Au-coated samples were then introduced to SEM Instrument (S-4700, Hitachi Co., Tokyo, Japan). High-resolution images of the cross sections were taken at a magnification of 100X at 5 kV.

4.2.6 Statistical analysis

All the experiments were conducted in duplicate, and the data were statistically analyzed using SAS® University edition (Proc Glimmax; SAS studio 9.4) using ANOVA with Tukey's test as posthoc analysis to identify significant differences between each sample group ($P < 0.05$).

4.3 Results and discussions

4.3.1 Moisture content and water activity

The moisture content and water activity of freeze dried PPI gels prepared using DW and PAMB are presented in Table 4.1. ARG90 had significantly higher moisture content and water activity while DW and ARG80 had statistically similar moisture content and water activity. The moisture content and the water activity of the freeze-dried samples determine the storage stability (Ciurzyńska and Lenart, 2011). Water activity also plays a significant role in the oxidative deterioration of freeze-dried plant proteins.

Table 4.1 Moisture content and water activity of freeze dried PPI

Sample	Moisture Content	Water Activity (a_w)
ARG80	6.142 ± 0.122^{b}	0.235 ± 0.013^{b}
ARG90	6.704 ± 0.270^{a}	0.264 ± 0.013^{a}
DW	5.780 ± 0.281^{b}	0.215 ± 0.022^{b}

Values are expressed as the mean ± standard deviation of two replicates. Alphabets a,b, within the same column indicate values that are significantly different ($p<0.05$).

4.3.2 Textural properties

The textural properties of freeze dried 3D-printed PPI gels are presented in Table 4.2. Critical textural properties such as hardness, fracturability, adhesiveness, chewiness, and cohesiveness were tested for each sample. The adhesiveness, chewiness, and cohesiveness were statistically

similar for all three samples, indicating no significant effect of PAMB in any of these properties. On the other hand, a significant difference was noted in the hardness values of the freeze dried ARG80 and DW gels i.e., the hardness was significantly lower for the DW sample compared to ARG80 sample.

For instance, with the incorporation of PAMB water for the production of PPI gels, the hardness of freeze dried PPI gels increased significantly from 2593.4 ± 1010.0 g (DW) to 3704.8 ± 387.2 g (ARG90) and 4239.7 ± 890.4 g (ARG80). A similar observation was noted in the case of the fracturability of the samples, with the value increasing with the incorporation of PAMB. The fracturability of PPI samples significantly increased ($p<0.05$) with the incorporation of PAMB, from 515.6 ± 420.0 (DW) to 2545.1 ± 571.8 (ARG90) and 2752.0± 1961.9 (ARG80).

These results are similar to the one obtained by Chen et al. (2020) when investigating the effect of cold plasma on high-protein wheat noodles. This research indicated a significant increase in the hardness of noodles that underwent cold plasma treatment. At the same time, some properties, such as adhesiveness and chewiness, did not exhibit a significant increase despite cold plasma treatment. Similar results were also cited by Ghribi et al. (2015), where freeze drying of chickpea proteins enhanced the hardness, while properties such as cohesiveness and adhesiveness remained statistically identical. Another study that employed a combination of cold plasma and vacuum freeze drying on jujube fruit slices indicated that the hardness and fracturability of the fruit remained statistically similar to the control samples (Yuan et al., 2022).

Table 4.2 Texture properties of freeze dried 3D printed pea protein gels

Sample	Hardness (g)	Fracturability (g)	Adhesiveness (g.s)	Chewiness (g.s)	Cohesiveness
ARG90	3704 ± 387[ba]	2545 ± 571 [a]	0.48 ± 0.1[a]	20.07 ± 22.9 [a]	0.03 ± 0.02 [a]
ARG80	4239 ± 890[a]	2751 ± 1961[a]	0.50 ± 0.1 [a]	8.38 ± 4.2 [a]	0.02 ± 0.01 [a]
DW	2593 ± 1009[b]	515.62 ± 419.9 [b]	0.35 ± 0.1[a]	13.35 ± 12.5 [a]	0.02 ± 0.01 [a]

Values are the Mean ± SD of two independent measurements. Alphabets a,b, and c within the same column indicate values that are significantly different statistically.

Even though PAMB water has an incremental effect on both the hardness and fracturability of the freeze dried pea protein isolates, it is to be noted that an increase in hardness is acceptable in food texture (Kim et al., 2011). In contrast, increased fracturability might only favour a few food products. An increased hardness indicates an increased food resistance to penetration by an externally applied force (Peng et al., 2002). An increased fracturability shows a higher tendency of the food to break or crumble, thereby offering a lower resistance to deformation and undergoing structural changes when pressure is applied (Peleg, 2019). Breakfast cereals are characterized by an increased hardness and fracturability, which indicate a potential application area for freeze dried PPI gels.

4.3.3 Scanning electron microscopy

The scanning electron microscopy images of freeze dried 3D-printed pea protein gels are presented in Figure 4.1. A change in the microstructure of the samples in various processing stages, such as suspension, gelation, and 3D printing, were observed. In the case of DW, the PPI suspension exhibited a compact and firm structure with a heterogeneous surface (Fig 4.1 A), while ARG80

and ARG90 suspensions (Fig 4.1 B, C) had increasingly visible pores. This change in microstructure, even before applying gelation and 3D printing, indicates that PAMB affected protein aggregation. A similar observation regarding protein aggregation with the application of atmospheric cold plasma was observed on fruit products (Yuan et al., 2022), animal proteins (Gong et al., 2021; Luo et al., 2020), and plant proteins (Rahman and Lamsal, 2023; Zhang et al., 2021) in earlier studies.

With the application of heat gelation and 3D printing, the morphology of protein underwent a prominent change in the case of ARG80 (Figure 4.1 E, H) and ARG90 (Figure 4.1 F, I), compared to DW (Figure 4.1 D, G). A weak gel network was observed in the case of DW and the pores were uneven and unequally distributed through the surface, indicating weak protein aggregation. In ARG80 and ARG90 samples, the formation of robust 3D gel networks with regular interconnective pores was observed. For ARG90 samples, the pore size increased, and the structure was more homogeneous than in the case of ARG80, indicating the formation of a solid gel.

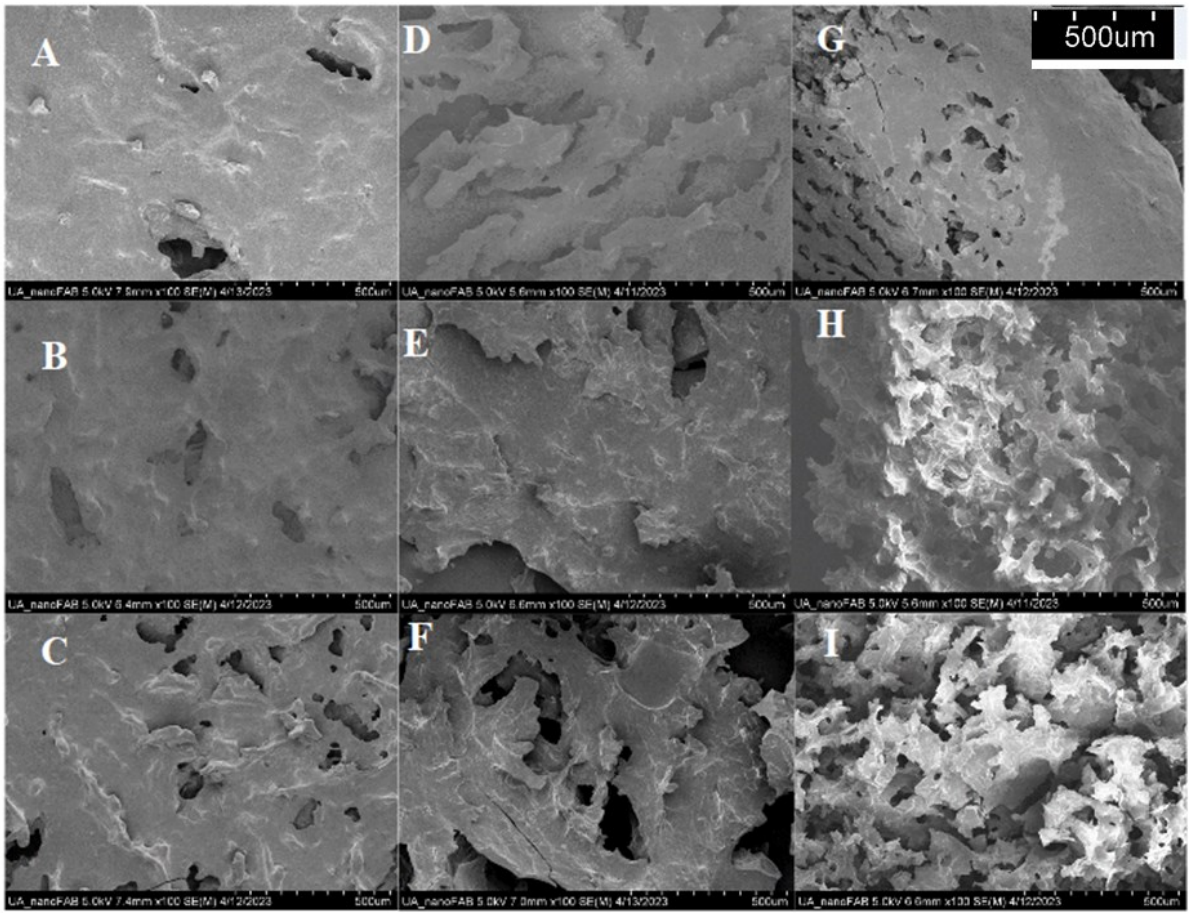

Figure 4.1 SEM images of freeze dried PPI suspensions, gels and 3D printed PPI gels.

The freeze dried PPI gels made from DW (A, D, and G), ARG80 (B, E, and H), and ARG90 (C, F, and I) during the different stages of preparation, i.e., as suspensions (A, B, and C), gels (D, E, and F) and 3D printed gels (G, H, and I). Images of the cross sections taken at a magnification of 100x at 5 kV. Images are of 500 μm in scale.

Similar observations related to the change in morphology and microstructure were reported for the heat-induced gelation of pea proteins pretreated by a modified pH-shifting method (Zhu et al., 2021). Earlier studies involving the direct treatment of cold plasma into pea protein isolate (Zhang et al., 2021; Bu et al., 2022) reported similar changes in morphology and microstructure. However, the present study's results indicate that indirect cold plasma treatments, such as the one generated using PAMB, can produce similar 3D gel networks and morphological changes in pea protein.

4.4 Conclusions

The hardness and fracturability of freeze dried 3D-printed PPI gels prepared by PAMB using feed gas containing 80% argon and 20% air were significantly different from those prepared using DW. Application of PAMB prepared using this gas combination increased the hardness and fracturability of freeze dried PPI gels, enabling a possible application in manufacturing protein-rich breakfast cereals. The microstructures of PPI gels demonstrated that the freeze dried PPI gels prepared using PAMB had better aggregation and gelation, forming compact 3D gel networks.

Chapter 5 Conclusions and recommendations

5.1 Conclusions

This MSc thesis research delves into the potential of pea protein isolate (PPI) as a suitable material for 3D printing. Traditionally, PPI is not viable for 3D printing and subsequent processing. However, by applying plasma-activated microbubble (PAMB) water and thermal gelation techniques, PPI exhibited improved 3D printing properties and excellent deformation stability upon storage.

In Chapter 3 of this study, using PAMB water to prepare pea protein suspensions resulted in the formation of PPI gels with better viscoelastic properties upon gelation. While the PPI suspensions made from distilled water formed weak, near stand-alone gels, PPI suspension made from PAMB water using specific gas combinations of argon and air resulted in stable stand-alone gels, which did not deform even after applying a small force with a glass rod.

Based on the rheological and mechanical properties analysis of the prepared gel, it has been determined that the PPI suspensions prepared with PAMB, gelled at 85°C for 60 min, had better gelation properties. The structural stability of the 3D printed PPI gels was enhanced when PAMB generated using a mixture of 80% argon and 20% air (ARG80) and 90% argon and 10% air (ARG90) were utilized. This improvement in these properties could be linked to the concentration and type of reactive oxygen and reactive nitrogen species present in PAMB.

In Chapter 4 of this study, freeze drying was evaluated as a possible post-processing operation for enhancing the storage properties of 3D-printed PPI gels. The application of PAMB to produce 3D-printed PPI gels impacted the microstructure of freeze dried PPI gels. The microstructures of PPI gels demonstrated that the freeze dried PPI gels prepared using PAMB had better aggregation and

gelation, forming compact 3D gel networks. Applying PAMB (using a mixture of 80% argon and 20% air (ARG80)) also increased the hardness and fracturability of freeze dried PPI gels.

Overall, this study demonstrated that plasma activated microbubble water can significantly improve pea proteins' functional properties. This study has also established the feasibility of utilizing pea protein as a sole ingredient in 3D food printing. Additionally, the protocol outlined in this study, which combines cold plasma, an emerging technology, with traditional technology of thermal gelation, can be applied to enhance the functional properties of other plant proteins.

5.2 Recommendations

The main objective of this study was to demonstrate the feasibility of applying cold plasma technology in combination with thermal gelation to enhance the functional properties of pea proteins. The following are areas that can be further investigated in the future:

1. This study mainly focussed on estimating the effect of reactive oxygen and reactive nitrogen species on pea protein. Further studies are required to estimate the contribution of reactive argon species that might have contributed to PPI gels' functionality and improved printability.
2. The present research estimated the effect of only two feed gases, air and argon, in PAMB water production and subsequent processing. Further research is required to estimate if gases like oxygen and nitrogen can also be utilized for similar purposes.
3. Since the study's primary objective was to assess the printability of pea protein suspension made out of different PAMB water gas compositions, the 3D model selected for the study is a primary cylinder. Further investigation into pea protein 3D printing with more complex shapes is required to estimate the possibilities of large-scale applications.

4. While estimating 3D printability, all the printing parameters, such as nozzle speed, printing temperature, and infill rate, were kept constant throughout the study. A future study is required to establish the impact of printing parameters on the 3D printability of pea protein.
5. Further studies on 3D printing of pea protein can be carried out to investigate the effect of possible additives such as beta glucan and xanthan gum.
6. This study established the possibility of freeze drying as a post-processing application for 3D-printed PPI gels. Since the encapsulation of bioactive compounds in pea proteins is gaining much scientific research, encapsulation of bioactive compounds can be included in this protocol after relevant studies.
7. This protocol of integrating plasma activated microbubble water and thermal gelation to enhance the functional properties can be applied to other emerging plant proteins (e.g., fava bean, lentil etc.).

References

Ahmadzadeh-Hashemi, S., Varidi, M., and Nooshkam, M. (2023). Hydro- and aerogels from quince seed gum and gelatin solutions. *Food Chemistry: X*, 19. https://doi.org/10.1016/j.fochx.2023.100813

Arif, M., and Pauls, K. P. (2018). Properties of plant proteins. In *Plant Bioproducts* (pp. 121–142). https://doi.org/10.1007/978-1-4939-8616-3_8

Assad Bustillos, M., Jonchère, C., Garnier, C., Réguerre, A. L., and Della Valle, G. (2020). Rheological and microstructural characterization of batters and sponge cakes fortified with pea proteins. *Food Hydrocolloids*, *101*, 105553 https://doi.org/10.1016/j.foodhyd.2019.105553

Avelar, Z., Vicente, A. A., Saraiva, J. A., and Rodrigues, R. M. (2021). The role of emergent processing technologies in tailoring plant protein functionality: New insights. *Trends in Food Science and Technology* (Vol. 113, pp. 219–231). https://doi.org/10.1016/j.tifs.2021.05.004

Ben-Harb, S., Irlinger, F., Saint-Eve, A., Panouillé, M., Souchon, I., and Bonnarme, P. (2020). Versatility of microbial consortia and sensory properties induced by the composition of different milk and pea protein-based gels. *LWT - Food Science and Technology, 118,* 108720. https://doi.org/10.1016/j.lwt.2019.108720

Bermudez-Aguirre, D. (2019a). Advances in the inactivation of microorganisms and viruses in food and model systems using cold plasma. *Advances in Cold Plasma Applications for Food Safety and Preservation* (pp. 49–91). https://doi.org/10.1016/B978-0-12-814921-8.00002-5

Bermudez-Aguirre, D. (2019b). Disinfection of high-moisture food using cold plasma. *Advances in Cold Plasma Applications for Food Safety and Preservation* (pp. 147–183). https://doi.org/10.1016/B978-0-12-814921-8.00005-0

Bhatta, S., Janezic, T. S., and Ratti, C. (2020). Freeze drying of plant-based foods. *Foods* (Vol. 9, Issue 1, 87). https://doi.org/10.3390/foods9010087

Bu, F., Feyzi, S., Nayak, G., Mao, Q., Kondeti, V. S. S. K., Bruggeman, P., Chen, C., and Ismail, B. P. (2023). Investigation of novel cold atmospheric plasma sources and their impact on the structural and functional characteristics of pea protein. *Innovative Food Science and Emerging Technologies*, *83,* 103248. https://doi.org/10.1016/j.ifset.2022.103248

Bu, F., Nayak, G., Bruggeman, P., Annor, G., and Ismail, B. P. (2022). Impact of plasma reactive species on the structure and functionality of pea protein isolate. *Food Chemistry*, *371*, 131135. https://doi.org/10.1016/j.foodchem.2021.131135

Chen, X. huan, Zhang, M., Teng, X. xiu, and Mujumdar, A. S. (2022). Internal structure design for improved shape fidelity and crispness of 3D printed pumpkin-based snacks after freeze drying . *Food Research International*, *157*, 111220. https://doi.org/10.1016/j.foodres.2022.111220

Chuanxing, F., Qi, W., Hui, L., Quancheng, Z., and Wang, M. (2018). Effects of Pea Protein on the Properties of Potato Starch-Based 3D Printing Materials. *International Journal of Food Engineering*, *14*(3), 297. https://doi.org/10.1515/ijfe-2017-0297

Ciurzyńska, A., Lenart, A., and Greda, K. J. (2014). Effect of pre-treatment conditions on content and activity of water and colour of freeze dried pumpkin. *LWT - Food Science and Technology*, *59*(2P1), 1075–1081. https://doi.org/10.1016/j.lwt.2014.06.035

Cui, L., Kimmel, J., Zhou, L., Chen, B., and Rao, J. (2021). Improving the functionality of pea protein isolate through co-spray drying with emulsifying salt or disaccharide. *Food Hydrocolloids*, *113*, 106534. https://doi.org/10.1016/j.foodhyd.2020.106534

Cui, L., Kimmel, J., Zhou, L., Rao, J., and Chen, B. (2020). Combining solid dispersion-based spray drying with cyclodextrin to improve the functionality and mitigate the beany odor of pea protein isolate. *Carbohydrate Polymers*, *245*, 116546 https://doi.org/10.1016/j.carbpol.2020.116546

Dankar, I., Haddarah, A., Omar, F. E. L., Sepulcre, F., and Pujolà, M. (2018). 3D printing technology: The new era for food customization and elaboration. *Trends in Food Science and Technology* (Vol. 75, pp. 231–242). https://doi.org/10.1016/j.tifs.2018.03.018

Detzel, A., Krüger, M., Busch, M., Blanco-Gutiérrez, I., Varela, C., Manners, R., Bez, J., and Zannini, E. (2022). Life cycle assessment of animal-based foods and plant-based protein-rich alternatives: an environmental perspective. *Journal of the Science of Food and Agriculture*, *102*(12), 5098–5110. https://doi.org/10.1002/jsfa.11417

FAOSTAT. (2023). Food and Agriculture Organization of the United Nations, Crop and Livestock Production Statistics. https://www.fao.org/faostat/en/#data/QCL

Feizollahi, E., Basu, U., Fredua-Agyeman, R., Jeganathan, B., Tonoyan, L., Strelkov, S. E., Vasanthan, T., Siraki, A. G., and Roopesh, M. S. (2023). Effect of plasma-activated water bubbles on *Fusarium graminearum,* deoxynivalenol, and germination of naturally infected barley during steeping. *Toxins*, *15*(2), 124 https://doi.org/10.3390/toxins15020124

Feizollahi, E., Misra, N. N., and Roopesh, M. S. (2020). Factors influencing the antimicrobial efficacy of Dielectric Barrier Discharge (DBD) Atmospheric Cold Plasma (ACP) in food processing applications. *Critical Reviews in Food Science and Nutrition*. *61(4),* 666-689. https://doi.org/10.1080/10408398.2020.1743967

Ferawati, F., Zahari, I., Barman, M., Hefni, M., Ahlström, C., Witthöft, C., and Östbring, K. (2021). High-moisture meat analogues produced from yellow pea and faba bean protein isolates/concentrate: Effect of raw material composition and extrusion parameters on texture properties. *Foods*, *10*(4), 843. https://doi.org/10.3390/foods10040843

Franceschinis, L., Salvatori, D. M., Sosa, N., and Schebor, C. (2014). Physical and functional properties of blackberry freeze- and spray-dried powders. *Drying Technology*, *32*(2), 197–207. https://doi.org/10.1080/07373937.2013.814664

Gao, K., Zha, F., Yang, Z., Rao, J., and Chen, B. (2022). Structure characteristics and functionality of water-soluble fraction from high-intensity ultrasound treated pea protein isolate. *Food Hydrocolloids*, *125*, 107409. https://doi.org/10.1016/j.foodhyd.2021.107409

Gao, Y., Francis, K., and Zhang, X. (2022). Review on formation of cold plasma activated water (PAW) and the applications in food and agriculture. *Food Research International*, *157*. https://doi.org/10.1016/j.foodres.2022.111246

Gao, Y., Li, M., Sun, C., and Zhang, X. (2022). Microbubble-enhanced water activation by cold plasma. *Chemical Engineering Journal*, *446*, 137318 https://doi.org/10.1016/j.cej.2022.137318

Ge, J., Sun, C. X., Corke, H., Gul, K., Gan, R. Y., and Fang, Y. (2020). The health benefits, functional properties, modifications, and applications of pea (*Pisum sativum L.)* protein: Current status, challenges, and perspectives. *Comprehensive Reviews in Food Science and Food Safety*, *19*(4), 1835–1876. https://doi.org/10.1111/1541-4337.12573

Ghribi, A. M., Gafsi, I. M., Blecker, C., Danthine, S., Attia, H., & Besbes, S. (2015). Effect of drying methods on physico-chemical and functional properties of chickpea protein concentrates. *Journal of Food Engineering*, *165*, 179 188. https://doi.org/10.1016/j.jfoodeng.2015.06.021

Godoi, F. C., Bhandari, B. R., Prakash, S., and Zhang, M. (2018). An introduction to the principles of 3D food printing. In *Fundamentals of 3D Food Printing and Applications* (pp. 1–18). https://doi.org/10.1016/B978-0-12-814564-7.00001-8

Gong, W., Guo, X., Huang, H., Li, X., Xu, Y., & Hu, J. (2021). Structural characterization of modified whey protein isolates using cold plasma treatment and its applications in emulsion oleogels. *Food Chemistry, 356,* 129703. https://doi.org/10.1016/j.foodchem.2021.129703

Guiné, R. P. F., and Barroca, M. J. (2012). Effect of drying treatments on texture and color of vegetables (pumpkin and green pepper). *Food and Bioproducts Processing*, *90*(1), 58–63. https://doi.org/10.1016/j.fbp.2011.01.003

Guo, D., Liu, H., Zhou, L., Xie, J., and He, C. (2021). Plasma-activated water production and its application in agriculture. *Journal of the Science of Food and Agriculture* (Vol. 101, Issue 12, pp. 4891–4899). https://doi.org/10.1002/jsfa.11258

Hawlader, M. N. A., Perera, C. O., Tian, M., and Yeo, K. L. (2006). Drying of guava and papaya: Impact of different drying methods. *Drying Technology*, *24*(1), 77–87. https://doi.org/10.1080/07373930500538725

Jiang, Q., Zhang, M., and Mujumdar, A. S. (2022). Novel evaluation technology for the demand characteristics of 3D food printing materials: a review. *Critical Reviews in Food Science and Nutrition* (Vol. 62, Issue 17, pp. 4669–4683). https://doi.org/10.1080/10408398.2021.1878099

Kaleda, A., Talvistu, K., Vaikma, H., Tammik, M. L., Rosenvald, S., and Vilu, R. (2021). Physicochemical, textural, and sensorial properties of fibrous meat analogs from oat-pea protein blends extruded at different moistures, temperatures, and screw speeds. *Future Foods*, *4*, 100092. https://doi.org/10.1016/j.fufo.2021.100092

Kaur, M., and Singh, N. (2007). Characterization of protein isolates from different Indian chickpea (Cicer arietinum L.) cultivars. *Food Chemistry*, *102*(1), 366–374. https://doi.org/10.1016/j.foodchem.2006.05.029

Klost, M., Brzeski, C., & Drusch, S. (2020). Effect of protein aggregation on rheological properties of pea protein gels. *Food Hydrocolloids, 108,* 106036. https://doi.org/10.1016/j.foodhyd.2020.106036

Kim, E. H., Corrigan, V. K., Wilson, A. J., Waters, I. R., Hedderley, D. I., & Morgenstern, M. P. (2011). Fundamental fracture properties associated with sensory hardness of brittle solid foods. *Journal of Texture Studies, 43(1)*, 49-62. https://doi.org/10.1111/j.1745-4603.2011.00316.x

Kim, H. W., Bae, H., and Park, H. J. (2017). Classification of the printability of selected food for 3D printing: Development of an assessment method using hydrocolloids as reference material. *Journal of Food Engineering*, *215*, 23–32. https://doi.org/10.1016/j.jfoodeng.2017.07.017

Kim, H. W., Lee, J. H., Park, S. M., Lee, M. H., Lee, I. W., Doh, H. S., and Park, H. J. (2018). Effect of hydrocolloids on rheological properties and printability of vegetable inks for 3d food printing. *Journal of Food Science*, *83*(12), 2923–2932. https://doi.org/10.1111/1750-3841.14391

Kim, Y., Kim, H. W., and Park, H. J. (2021). Effect of pea protein isolate incorporation on 3D printing performance and tailing effect of banana paste. *LWT - Food Science and Technology*, *150*, 111916. https://doi.org/10.1016/j.lwt.2021.111916

Kumar, M., Tomar, M., Punia, S., Dhakane-Lad, J., Dhumal, S., Changan, S., Senapathy, M., Berwal, M. K., Sampathrajan, V., Sayed, A. A. S., Chandran, D., Pandiselvam, R., Rais, N., Mahato, D. K., Udikeri, S. S., Satankar, V., Anitha, T., Reetu, Radha, Kennedy, J. F. (2022). Plant-based proteins and their multifaceted industrial applications. *LWT - Food Science and Technology*, *154*, 112620. https://doi.org/10.1016/j.lwt.2021.112620

Kumar, P. K., Sivabalan, S., Parhi, A., and Sablani, S. S. (2022). Modification of pea protein isolate functionality by freeze–thaw cycling. *Journal of Food Measurement and Characterization*, *16*(1), 162–170. https://doi.org/10.1007/s11694-021-01151-x

Kuo, C. C., Clark, S., Qin, H., and Shi, X. (2022). Development of a shelf-stable, gel-based delivery system for probiotics by encapsulation, 3D printing, and freeze drying. *LWT - Food Science and Technology*, *157,* 113075. https://doi.org/10.1016/j.lwt.2022.113075

Lam, A. C. Y., Can Karaca, A., Tyler, R. T., and Nickerson, M. T. (2018). Pea protein isolates: Structure, extraction, and functionality. *Food Reviews International* (Vol. 34, Issue 2, pp. 126–147). https://doi.org/10.1080/87559129.2016.1242135

Le Tohic, C., O'Sullivan, J. J., Drapala, K. P., Chartrin, V., Chan, T., Morrison, A. P., Kerry, J. P., and Kelly, A. L. (2018). Effect of 3D printing on the structure and textural properties of processed cheese. *Journal of Food Engineering*, *220*, 56–64. https://doi.org/10.1016/j.jfoodeng.2017.02.003

Li, X., Fan, L., Liu, Y., and Li, J. (2021). New insights into food O/W emulsion gels: Strategies of reinforcing mechanical properties and outlook of being applied to food 3D printing. *Critical Reviews in Food Science and Nutrition*, *63(11),* 1564-1586 https://doi.org/10.1080/10408398.2021.1965953

Lille, M., Nurmela, A., Nordlund, E., Metsä-Kortelainen, S., & Sozer, N. (2018). Applicability of protein and fiber-rich food materials in extrusion-based 3D printing. *Journal of Food Engineering*, *220*, 20- 27. https://doi.org/10.1016/j.jfoodeng.2017.04.034

Lipton, J. I. (2017). Printable food: the technology and its application in human health. *Current Opinion in Biotechnology* (Vol. 44, pp. 198–201). https://doi.org/10.1016/j.copbio.2016.11.015

Liu, Y., Liu, D., Wei, G., Ma, Y., Bhandari, B., and Zhou, P. (2018). 3D printed milk protein food simulant: Improving the printing performance of milk protein concentration by incorporating whey protein isolate. *Innovative Food Science and Emerging Technologies*, *49*, 116–126. https://doi.org/10.1016/j.ifset.2018.07.018

Liu, Y., Yu, Y., Liu, C., Regenstein, J. M., Liu, X., and Zhou, P. (2019). Rheological and mechanical behavior of milk protein composite gel for extrusion-based 3D food printing. *LWT - Food Science and Technology*, *102*, 338–346. https://doi.org/10.1016/j.lwt.2018.12.053

Luo, J., Muhammad Nasiru, M., Yan, W., Zhuang, H., Zhou, G., and Zhang, J. (2020). Effects of dielectric barrier discharge cold plasma treatment on the structure and binding capacity of aroma compounds of myofibrillar proteins from dry-cured bacon. *LWT - Food Science and Technology*, *117*, 108606. https://doi.org/10.1016/j.lwt.2019.108606

Mai-Prochnow, A., Zhou, R., Zhang, T., Ostrikov, K. (Ken), Mugunthan, S., Rice, S. A., and Cullen, P. J. (2021). Interactions of plasma-activated water with biofilms: inactivation, dispersal effects and mechanisms of action. *npj Biofilms and Microbiomes* (Vol. 7, Issue 1), 180. https://doi.org/10.1038/s41522-020-00180-6

Majumdar, A. S. (2007). *Handbook of Industrial Drying- Third Edition* (A. S. Majumdar, Ed.; Third). https://www.taylorfrancis.com/books/mono/10.1201/b17208/handbook-industrial-drying-arun-mujumdar

Małecki, J., Muszyński, S., and Sołowiej, B. G. (2021). Proteins in food systems—bionanomaterials, conventional and unconventional sources, functional properties, and development opportunities. *Polymers, 13(15),* 2506. https://doi.org/10.3390/polym13152506

Mantihal, S., Kobun, R., and Lee, B. B. (2020). 3D food printing of as the new way of preparing food: A review. *International Journal of Gastronomy and Food Science, 22*, 260. https://doi.org/10.1016/j.ijgfs.2020.100260

Mantihal, S., Prakash, S., Godoi, F. C., and Bhandari, B. (2019). Effect of additives on thermal, rheological and tribological properties of 3D printed dark chocolate. *Food Research International*, *119*, 161–169. https://doi.org/10.1016/j.foodres.2019.01.056

Manzocco, L., Plazzotta, S., Powell, J., de Vries, A., Rousseau, D., and Calligaris, S. (2021). Structural characterisation and sorption capability of whey protein aerogels obtained by freeze drying or supercritical drying. *Food Hydrocolloids*, *122*,107117 https://doi.org/10.1016/j.foodhyd.2021.107117

Meda, L., and Ratti, C. (2005). Rehydration of freeze dried strawberries at varying temperatures. *Journal of Food Process Engineering*, *28*(3), 233–246. https://doi.org/10.1111/j.1745-4530.2005.00404.x

Mirmoghtadaie, L., Shojaee Aliabadi, S., and Hosseini, S. M. (2016). Recent approaches in physical modification of protein functionality. *Food Chemistry* (Vol. 199, pp. 619–627). https://doi.org/10.1016/j.foodchem.2015.12.067

Misra, N. N., Yepez, X., Xu, L., and Keener, K. (2019). In-package cold plasma technologies. *Journal of Food Engineering* (Vol. 244, pp. 21–31). Elsevierhttps://doi.org/10.1016/j.jfoodeng.2018.09.019

Moreno, H. M., Domínguez-Timón, F., Díaz, M. T., Pedrosa, M. M., Borderías, A. J., & Tovar, C. A. (2020). Evaluation of gels made with different commercial pea protein isolate: Rheological, structural and functional properties. Food Hydrocolloids, 99, 105375. https://doi.org/10.1016/j.foodhyd.2019.105375

Munialo, C. D. (2023). A review of alternative plant protein sources, their extraction, functional characterisation, application, nutritional value and pinch points to being the solution to sustainable food production. *International Journal of Food Science and Technology, 29(3), 16467* https://doi.org/10.1111/ijfs.16467

Munzenmayer, P., Ulloa, J., Pinto, M., Ramirez, C., Valencia, P., Simpson, R., and Almonacid, S. (2020). Freeze drying of blueberries: Effects of carbon dioxide (CO_2) laser perforation as skin pretreatment to improve mass transfer, primary drying time, and quality. *Foods*, *9*(2), 211. https://doi.org/10.3390/foods9020211

Nicolai, T., and Chassenieux, C. (2019). Heat-induced gelation of plant globulins. *Current Opinion in Food Science* (Vol. 27, pp. 18–22). https://doi.org/10.1016/j.cofs.2019.04.005

Nindo, C. I., Sun, T., Wang, S. W., Tang, J., and Powers, J. R. (2003). Evaluation of drying technologies for retention of physical quality and antioxidants in asparagus (*Asparagus officinalis*, L.). *LWT - Food Science and Technology*, *36*(5), 507–516. https://doi.org/10.1016/S0023-6438(03)00046-X

Nowak, D., & Jakubczyk, E. (2020). The freeze-drying of foods—The characteristic of the process course and the effect of its parameters on the physical properties of food materials. *Foods, 9(10),* 1488. https://doi.org/10.3390/foods9101488

O'Kane, F. E., Vereijken, J. M., Gruppen, H., and Van Boekel, M. A. J. S. (2005). Gelation behavior of protein isolates extracted from 5 cultivars of *Pisum sativum* L. *Journal of Food Science*, *70*(2), C132-C137 https://doi.org/10.1111/j.1365-2621.2005.tb07073.x

Omura, M. H., de Oliveira, A. P. H., Soares, L. de S., Coimbra, J. S. dos R., de Barros, F. A. R., Vidigal, M. C. T. R., Baracat-Pereira, M. C., and de Oliveira, E. B. (2021). Effects of protein concentration during ultrasonic processing on physicochemical properties and techno-functionality of plant food proteins. *Food Hydrocolloids*, *113*, 106457. https://doi.org/10.1016/j.foodhyd.2020.106457

Owusu-Ansah, Y. J., and Mc curdy, S. M. (1991). Pea proteins: A review of chemistry, technology of production, and utilization. *Food Reviews International* (Vol. 7, Issue 1, pp. 103–134). https://doi.org/10.1080/87559129109540903

Park, S. J., Kim, T., and Baik, B. K. (2010). Relationship between proportion and composition of albumins, and in vitro protein digestibility of raw and cooked pea seeds (*Pisum sativum* L.). *Journal of the Science of Food and Agriculture*, *90*(10), 1719–1725. https://doi.org/10.1002/jsfa.4007

Peleg, M. (2019). The instrumental texture profile analysis revisited. *Journal of Texture Studies* (Vol. 50, Issue 5, pp. 362–368). https://doi.org/10.1111/jtxs.12392

Peng, Y., Sun, X., Carson, L., & Setser, C. (2002). Food hardness and fracturability assessment by an electronic sensing system. *Journal of Texture Studies, 33(2)*, 135-148. https://doi.org/10.1111/j.1745-4603.2002.tb01340.x

Pérez, B., Nykvist, H., Brøgger, A. F., Larsen, M. B., & Falkeborg, M. F. (2019). Impact of macronutrients printability and 3D-printer parameters on 3D-food printing: A review. *Food Chemistry*, *287*, 249-257. https://doi.org/10.1016/j.foodchem.2019.02.090

Picout, D. R., & Ross-Murphy, S. B. (2003). Rheology of Biopolymer solutions and gels. *The Scientific World Journal*, *3*, 105-121. https://doi.org/10.1100/tsw.2003.15

Preethi, R., Moses, J., & Anandharamakrishnan, C. (2021). Effect of conductive hydro-drying on physiochemical and functional properties of two pulse protein extracts: Green Gram (Vigna radiata) and Black Gram (Vigna Mungo). *Food Chemistry*, *343*, 128551. https://doi.org/10.1016/j.foodchem.2020.1285

Qian, J., Wang, Y., Zhuang, H., Yan, W., Zhang, J., & Luo, J. (2021). Plasma activated water-induced formation of compact chicken myofibrillar protein gel structures with intrinsically antibacterial activity. *Food Chemistry, 351*, 129278. https://doi.org/10.1016/j.foodchem.2021.129278

Rahman, M. M., and Lamsal, B. P. (2023). Effects of atmospheric cold plasma and high-power sonication on rheological and gelling properties of mung bean protein dispersions. *Food Research International*, *163*, 112265. https://doi.org/10.1016/j.foodres.2022.112265

Rao, N., Chu, X., Hadinoto, K., Angelina, Zhou, R., Zhang, T., Soltani, B., Bailey, C., Trujillo, F., Leslie, G., Prescott, S., Cullen, P., & Henderson, R. (2023). Algal cell inactivation and damage via cold plasma-activated bubbles: Mechanistic insights and process benefits. *Chemical Engineering Journal, 454,* 140304. https://doi.org/10.1016/j.cej.2022.140304

Regier, M., Mayer-Miebach, E., Behsnilian, D., Neff, E., and Schuchmann, H. P. (2005). Influences of drying and storage of lycopene-rich carrots on the carotenoid content. *Drying Technology*, *23*(4), 989–998. https://doi.org/10.1081/DRT-200054255

Rubio, L. A., Pérez, A., Ruiz, R., Guzmán, M. Á., Aranda-Olmedo, I., & Clemente, A. (2013). Characterization of pea (*Pisum sativum*) seed protein fractions. *Journal of the Science of Food and Agriculture, 94(2)*, 280-287. https://doi.org/10.1002/jsfa.6250

Sá, A. G. A., Moreno, Y. M. F., and Carciofi, B. A. M. (2019). Food processing for the improvement of plant proteins digestibility. *Critical Reviews in Food Science and Nutrition*. *60(20),* 3367-3386https://doi.org/10.1080/10408398.2019.1688249

Severini, C., Derossi, A., and Azzollini, D. (2016). Variables affecting the printability of foods: Preliminary tests on cereal-based products. *Innovative Food Science and Emerging Technologies*, *38*, 281–291. https://doi.org/10.1016/j.ifset.2016.10.001

Shanthakumar, P., Klepacka, J., Bains, A., Chawla, P., Dhull, S. B., & Najda, A. (2022). The current situation of pea protein and its application in the food industry. *Molecules, 27(16),* 5354. https://doi.org/10.3390/molecules27165354

Shevkani, K., Singh, N., Kaur, A., & Rana, J. C. (2015). Structural and functional characterization of kidney bean and field pea protein isolates: A comparative study. *Food Hydrocolloids*, *43*, 679-689. https://doi.org/10.1016/j.foodhyd.2014.07.024

Silva-Espinoza, M. A., Ayed, C., Foster, T., Del Mar Camacho, M., and Martínez-Navarrete, N. (2020). The impact of freeze drying conditions on the physico-chemical properties and bioactive compounds of a freeze dried orange puree. *Foods*, *9*(1), 32 https://doi.org/10.3390/foods9010032

Sim, S. Y. J., Srv, A., Chiang, J. H., and Henry, C. J. (2021). Plant proteins for future foods: A roadmap. In *Foods* (Vol. 10, Issue 8, pp 1967). https://doi.org/10.3390/foods10081967

Soni, A., Choi, J., and Brightwell, G. (2021). Plasma-activated water (PAW) as a disinfection technology for bacterial inactivation with a focus on fruit and vegetables. *Foods* (Vol. 10, Issue 1, pp 166). https://doi.org/10.3390/foods10010166

Statistics Canada. (2023). Canada: Outlook for principal field crops. *Agriculture and Agri-Food Canada.* https://agriculture.canada.ca/en/sector/crops/reports-statistics/canada-outlook-principal-field-crops-2023-08-18#a4

Sun, J., Zhou, W., Yan, L., Huang, D., and Lin, L. ya. (2018). Extrusion-based food printing for digitalized food design and nutrition control. *Journal of Food Engineering*, *220*, 1–11. https://doi.org/10.1016/j.jfoodeng.2017.02.028

Voon, S. L., An, J., Wong, G., Zhang, Y., and Chua, C. K. (2019). 3D food printing: a categorised review of inks and their development. *Virtual and Physical Prototyping* (Vol. 14, Issue 3, pp. 203–218). https://doi.org/10.1080/17452759.2019.1603508

Wadhave, A. A., Jadhav, A. I., and Arsul, V. A. (2014). Plant proteins applications: A review. *World Journal of Pharmacy and Pharmaceutical Sciences*, *3*(3), 702–712. www.wjpps.com

Xia, S., Xue, Y., Xue, C., Jiang, X., and Li, J. (2022). Structural and rheological properties of meat analogues from *Haematococcus pluvialis* residue-pea protein by high moisture extrusion. *LWT - Food Science and Technology*, *154*, 112756. https://doi.org/10.1016/j.lwt.2021.112756

Xiao, X., Zou, P. R., Hu, F., Zhu, W., and Wei, Z. J. (2023). Updates on plant-based protein products as an alternative to animal protein: technology, properties, and their health benefits. *Molecules* (Vol. 28, Issue 10, pp 4016) https://doi.org/10.3390/molecules28104016

Xu, P., and Tan, J. (2023). Inactivation and removal of *Klebsiella michiganensis* biofilm attached to the inner surfaces of piping by plasma-activated microbubble water (PMBW). *Innovative Food Science and Emerging Technologies*, *86*, 3360. https://doi.org/10.1016/j.ifset.2023.103360

Yang, C., Zhang, Z., Liu, L., Li, Y., Dong, X., and Chen, W. (2022). Fabrication of soy protein isolate/κ-carrageenan hydrogels for release control of hydrophilic compounds: Flax lignans. *International Journal of Biological Macromolecules*, *223*, 821–829. https://doi.org/10.1016/j.ijbiomac.2022.11.007

Yang, J., Mocking-Bode, H. C. M., van den Hoek, I. A. F., Theunissen, M., Voudouris, P., Meinders, M. B. J., and Sagis, L. M. C. (2022). The impact of heating and freeze or spray drying on the interface and foam stabilising properties of pea protein extracts: Explained by aggregation and protein composition. *Food Hydrocolloids*, *133*, 107913. https://doi.org/10.1016/j.foodhyd.2022.107913

Yu, X., Zhao, Z., Zhang, N., Yan, B., Gao, W., Huang, J., Zhao, J., Zhang, H., Chen, W., and Fan, D. (2022). Effects of preheating-induced denaturation treatments on the printability and instant curing property of soy protein during microwave 3D printing. *Food Chemistry*, *397*, 133682. https://doi.org/10.1016/j.foodchem.2022.133682

Yuan, L., Lao, F., Shi, X., Zhang, D., and Wu, J. (2022). Effects of cold plasma, high hydrostatic pressure, ultrasound, and high-pressure carbon dioxide pretreatments on the quality characteristics of vacuum freeze dried jujube slices. *Ultrasonics Sonochemistry*, *90*, 106219. https://doi.org/10.1016/j.ultsonch.2022.106219

Zhang, J. Y., Pandya, J. K., McClements, D. J., Lu, J., and Kinchla, A. J. (2022). Advancements in 3D food printing: a comprehensive overview of properties and opportunities. *Critical Reviews in Food Science and Nutrition* (Vol. 62, Issue 17, pp. 4752–4768) https://doi.org/10.1080/10408398.2021.1878103

Zhang, K., Zhao, M., Sun, D. W., and Tiwari, B. K. (2023). Correlation of plasma generated long-lived reactive species in aqueous and gas phases with different feeding gases. *Plasma Sources Science and Technology*, *32*(4), 684. https://doi.org/10.1088/1361-6595/acc684

Zhang, S., Huang, W., Feizollahi, E., Roopesh, M. S., and Chen, L. (2021). Improvement of pea protein gelation at reduced temperature by atmospheric cold plasma and the gelling mechanism study. *Innovative Food Science and Emerging Technologies*, *67*, 102567. https://doi.org/10.1016/j.ifset.2020.102567

Zhu, H. G., Tang, H. Q., Cheng, Y. Q., Li, Z. G., and Tong, L. T. (2021). Potential of preparing meat analogue by functional dry and wet pea (*Pisum sativum*) protein isolate. *LWT - Food Science and Technology*, *148*, 111702 https://doi.org/10.1016/j.lwt.2021.111702

Zhu, M., Dang, J., Dong, F., Zhong, R., Zhang, J., Pan, J., and Li, Y. (2023). Antimicrobial and cleaning effects of ultrasonic-mediated plasma-loaded microbubbles on *Enterococcus faecalis* biofilm: an in vitro study. *BMC Oral Health*, *23*(1), 2813. https://doi.org/10.1186/s12903-023-02813-6

Appendix I Mechanical properties of PPI PAMB gels at 80°C, 85°C and 90°C for 60 min

HEATING TEMPERATURE °C	PPI Gels	COMPRESSIVE STRESS kPa	COMPRESSIVE STRAIN mm/mm	YOUNG'S MODULUS kPa
90°C	DW	3.83 ± 0.18 ^{c}	0.23 ± 0.02 ^{c}	21.9 ± 2.70 ^{b}
	AIR100	4.96 ± 0.32 ^{ba}	0.24 ± 0.01 ^{cb}	25.89 ± 2.81 ^{ba}
	ARG90	4.23 ± 0.75 ^{a}	0.25 ± 0.01 ^{b}	21.77 ± 3.19 ^{b}
	ARG80	4.03 ± 0.81 ^{bc}	0.24 ± 0.02 ^{a}	29.28 ± 3.27 ^{a}
85°C	DW	2.57 ± 0.44 c	0.21 ± 0.01 ^{c}	18.15 ± 5.82 ^{b}
	AIR100	3.94 ± 0.40 ^{ba}	0.22 ± 0.03 ^{cb}	21.01 + 1.14 ^{ba}
	ARG90	4.76 ± 0.88 ^{a}	0.24 ± 0.02 ^{b}	24.91 ± 5.58 ^{b}
	ARG80	4.03 ± 0.81 ^{bc}	0.28 ± 0.03 ^{a}	21.59 ± 2.97 ^{a}
80°C	DW	2.45 ± 0.70 c	0.2 ± 0.01 ^{c}	13.42 ± 2.10 ^{b}
	AIR100	2.33 + 0.58 ^{ba}	0.21 ± 0.04 ^{cb}	15.65 ± 4.29 ^{ba}
	ARG90	3.39 ± 0.74 ^{a}	0.21 ± 0.03 ^{b}	16.29 ± 1.04 ^{b}
	ARG80	3.2 ± 0.28 ^{bc}	0.22 ± 0.02 ^{a}	17.33 ± 2.59 ^{a}

Appendix II Stress- Strain Curve Outputs of PPI Gels (Instron)

ARG80-30min

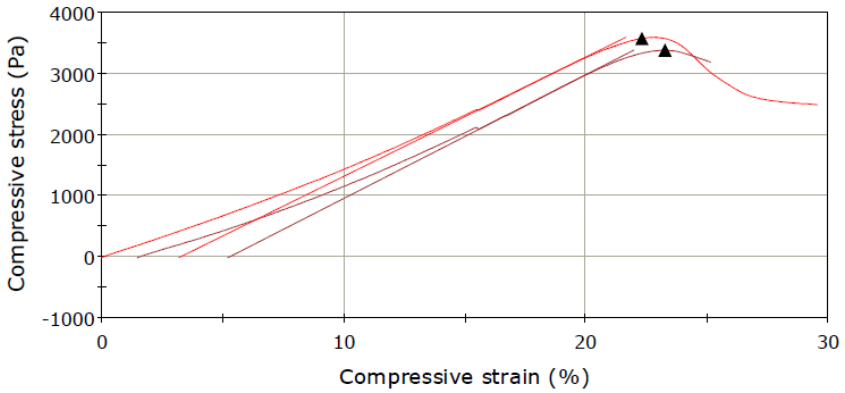

ARG90-30min

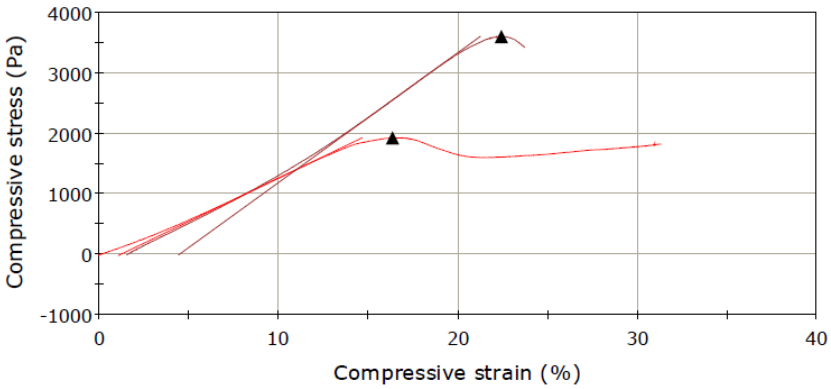

ARG100-30min

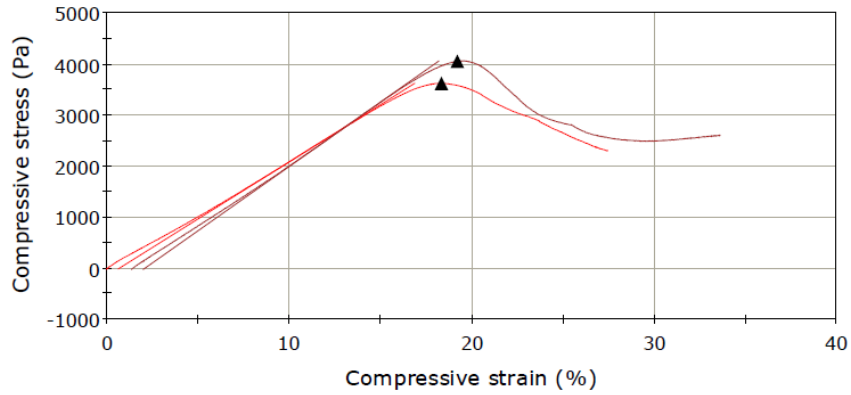

AIR100-30min

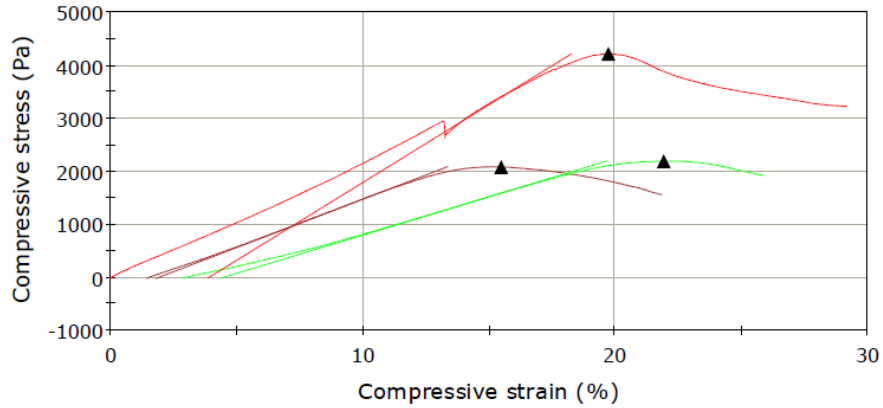

DW-30min

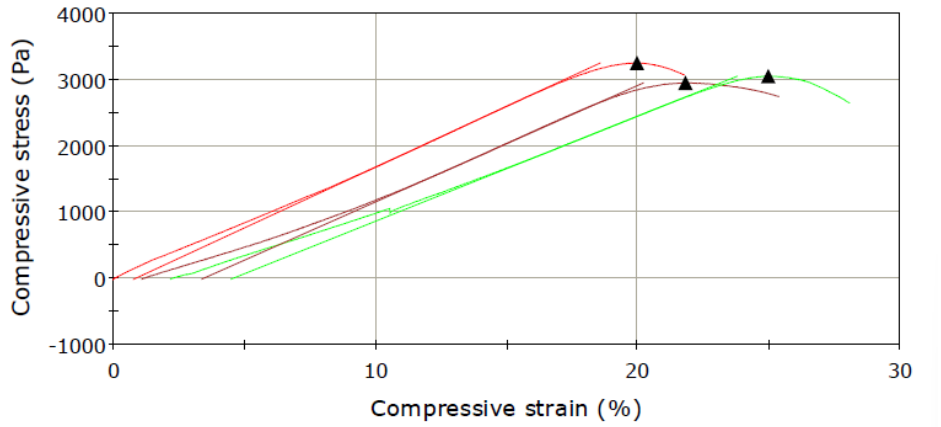

ARG80-60min

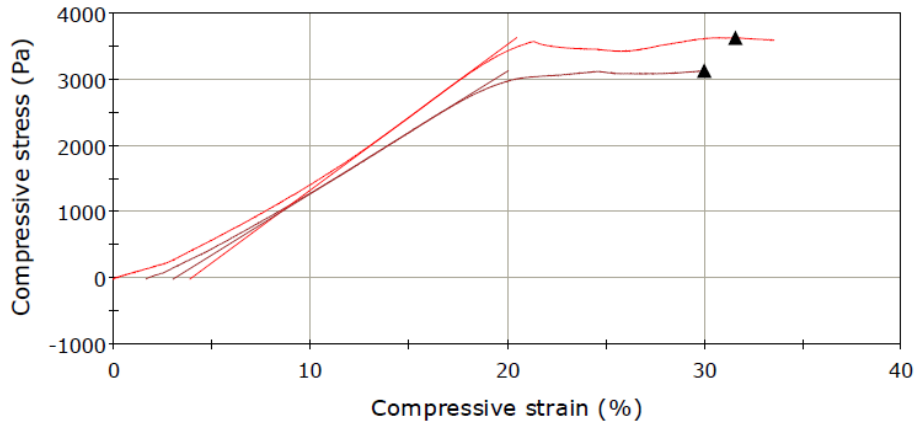

ARG90-60min

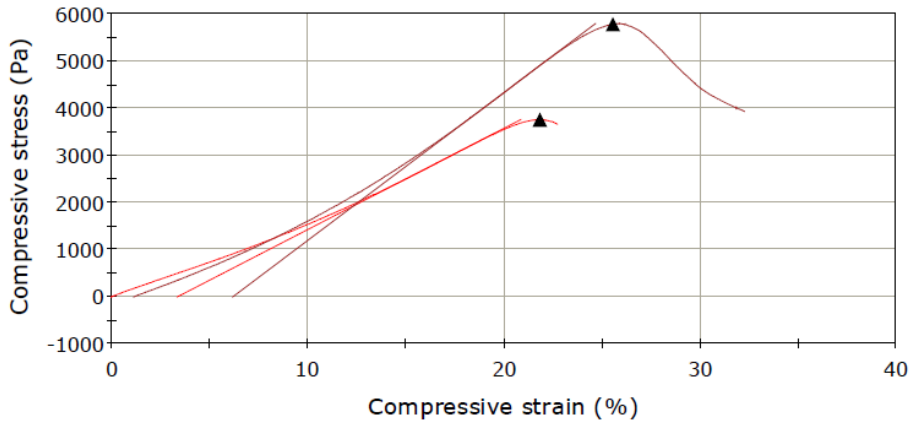

ARG100-60min

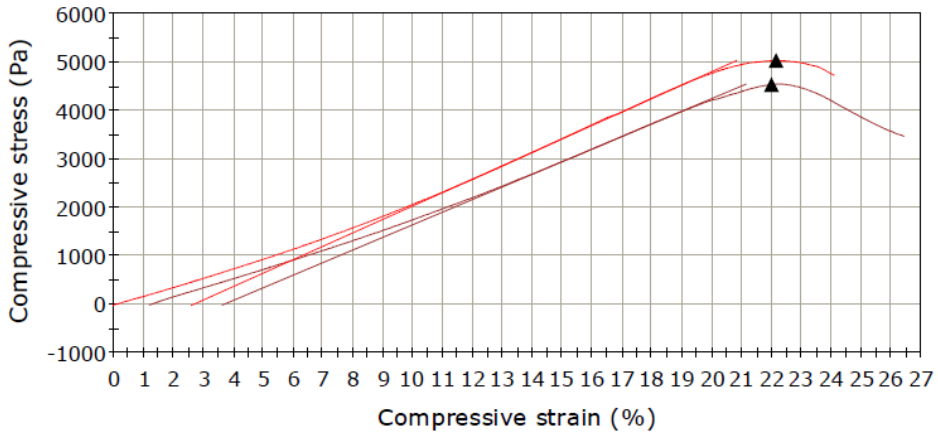

AIR100-60min

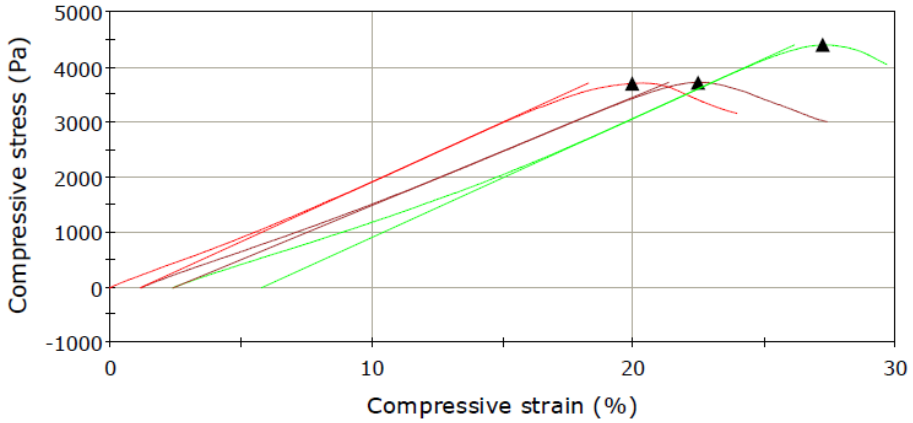

DW-60 min

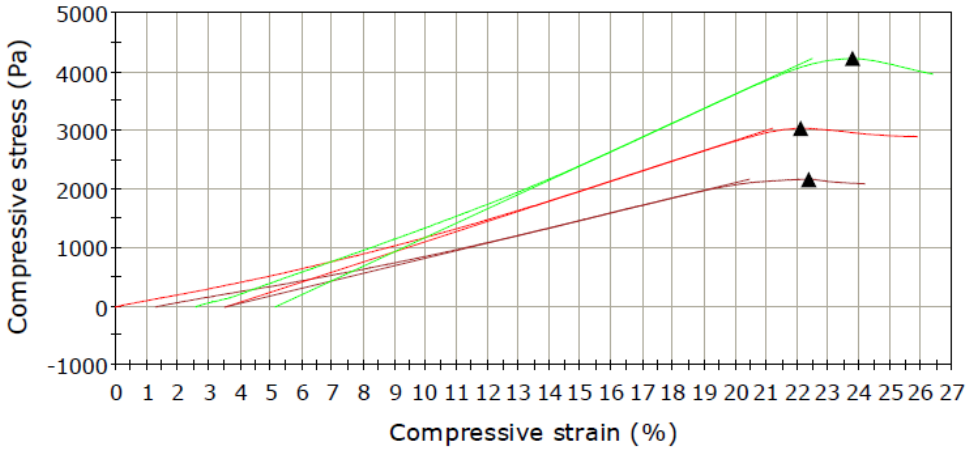

Appendix III Force-Time Curve of 3D Printed Freeze dried PPI Gels (Texture Profile Analyzer)

ARG80

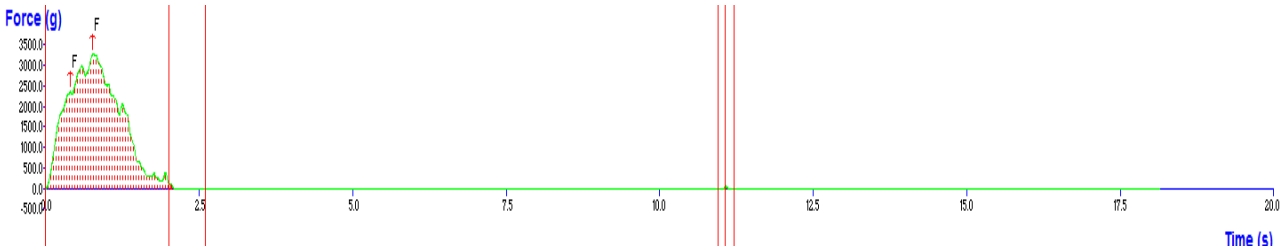

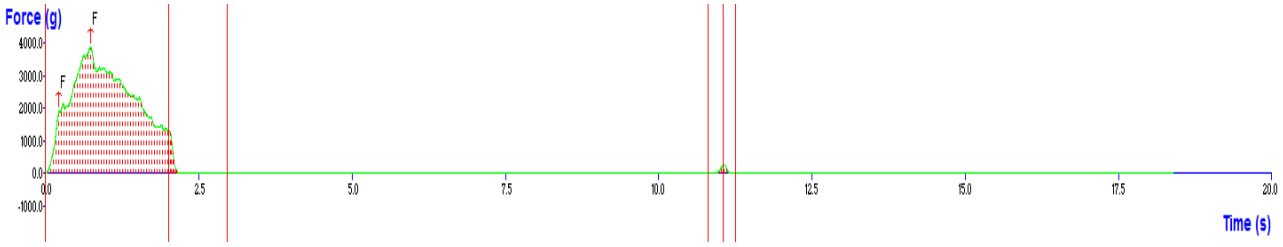

ARG90

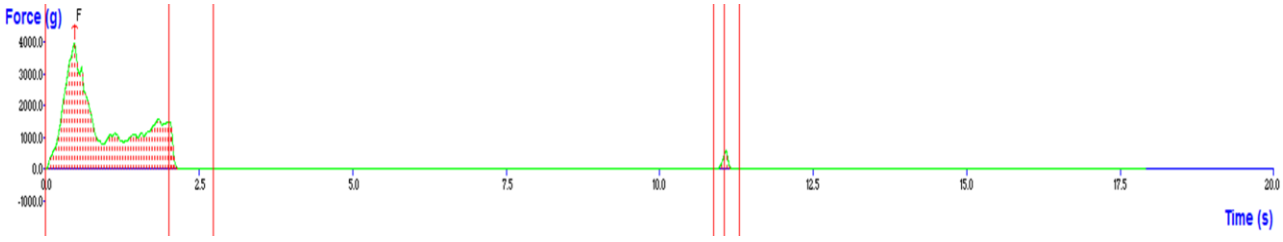

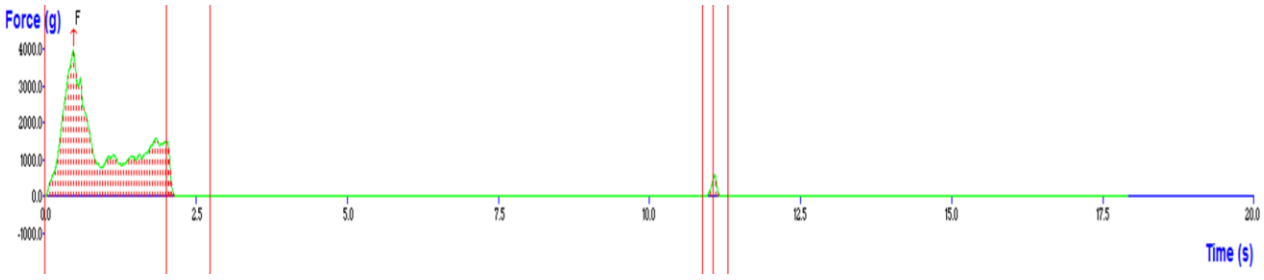

DW

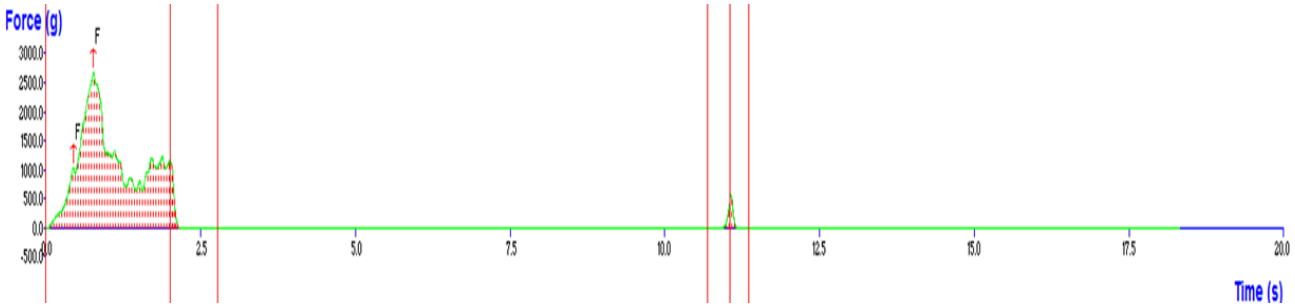
Force (g)
F
F
3000.0
2500.0
2000.0
1500.0
1000.0
500.0
0.0
-500.0
0.0
2.5
5.0
7.5
10.0
12.5
15.0
17.5
20.0
Time (s)

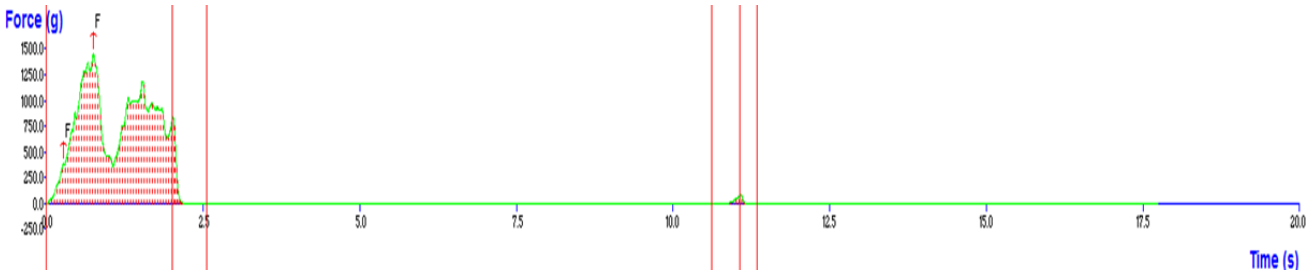
Force (g)
F
F
1500.0
1250.0
1000.0
750.0
500.0
250.0
0.0
-250.0
0.0
2.5
5.0
7.5
10.0
12.5
15.0
17.5
20.0
Time (s)